TÜRKİYE CUMHURİYETİ
ADANA ALPARSLAN TÜRKEŞ SCIENCE AND TECHNOLOGY UNIVERSITY

GRADUATE SCHOOL
DEPARTMENT OF BIOENGINEERING

DEVELOPMENT OF ANGIOTENSIN (II) IMPRINTED NANOPARTICLES

PIRIL ARISOY

MASTER OF SCIENCE

ADANA 2023

TÜRKİYE CUMHURİYETİ
ADANA ALPARSLAN TÜRKEŞ SCIENCE AND TECHNOLOGY UNIVERSITY

GRADUATE SCHOOL

DEPARTMENT OF BIOENGINEERING

DEVELOPMENT OF ANGIOTENSIN (II) IMPRINTED NANOPARTICLES

PIRIL ARISOY

MASTER OF SCIENCE

SUPERVISOR

PROF. DR. GÖZDE BAYDEMİR PEŞİNT

ADANA, 2023

DECLARATION OF CONFORMITY

In this thesis study, which was prepared following the thesis writing rules of Adana Alparslan Türkeş Science and Technology University Institute of Graduate School, I declare that I provide all the information, documents, evaluations and results in accordance with scientific ethics and moral codes without resorting to any means or assistance that would be contrary to scientific ethics and traditions. I also declare that I refer to all of the articles I used in this study with appropriate references and accept all moral and legal consequences if a situation is found contrary to my statement regarding my work.

23/06/2023

Pırıl ARISOY

ÖZET

ANJİYOTENSİN (II) BASKILANMIŞ NANOPARTİKÜLLERİN ÜRETİLMESİ

Pırıl ARISOY
Yüksek Lisans, Biyomühendislik Anabilim Dalı

Danışman: Prof. Dr. Gözde BAYDEMİR PEŞİNT
Haziran 2023, 74 sayfa

Anjiyotensin II (Ang II), vazokonstriksiyona ve kan basıncında artışa neden olan bir peptit hormonudur. Kan basıncını düzenleyen renin-anjiyotensin sisteminin bir parçasıdır. Ang II'nin kardiyovasküler denge üzerindeki rolü oldukça büyüktür. Bilimsel olarak kanıtlanmış kalp ve damar hastalıkları ile olan ilişkisi nedeniyle hastalıkların tespiti için kan serumunda önemli bir biyobelirteçtir. Moleküler baskılanmış polimerler (MIP), belirli bir hedef molekülün yüksek seçicilikle tanınmasını sağlayan afinite tabanlı polimerik destek malzemeleridir. Moleküler baskılama yöntemi, karmaşık bir ortamdan istenen molekülü (örn. protein, amino asit, peptit, iyon vb.) hızlı ve yüksek seçicilikle tanımak için çok sık kullanılan güvenilir bir tekniktir. Bu tez kapsamında sulu çözeltilerden Ang II tayini için miniemülsiyon polimerizasyon reaksiyonu ile Ang II baskılanmış nanopartiküller sentezlenmiştir. Hidroksietil metakrilat (HEMA) bazlı nanopartiküllerin (NP) hazırlanması için ikili faz karışımı hazırlanmıştır. Ang II baskılanmış (Ang II-MIP_{np}) ve baskılanmamış nanopartiküller (NIP_{np}) sentezlendikten sonra Zeta Boyut analizi, Taramalı Elektron mikroskobu (SEM), Geçirgen Elektron Mikroskobu (TEM) ve FTIR-ATR spektrofotometre ile karakterize edilmiştir. Daha sonra spesifik yüzey alanları hesaplanmıştır. NP'lerin ortalama partikül boyutu 50 nm olarak kaydedildi. Ang II-MIP_{np} ve NIP_{np}'in spesifik yüzey alanları sırasıyla 26903.4 ve 25868.9 m^2/g olarak hesaplanmıştır. %98 başarı oranı ile Ang II molekülleri, Ang II-MIP_{np}'de şablona özgü boşluklar oluşturmak için polimerik yapıdan başarılı bir şekilde serbest bırakılmıştır. Ardından, Ang II moleküllerinin sulu çözeltilerinden adsorpsiyonu, tanıma bölgelerine bağlanma kapasiteleri açısından incelenmiştir. NP'lerin Ang II adsorpsiyonunun hassas bir şekilde 50 pg/mL'ye kadar inebildiği bulunmuştur. Desorpsiyon için 0,5 M NaCl çözeltisi kullanılmış ve %98 geri kazanım sağlanmıştır. Adsorpsiyon-desorpsiyon döngüsü 10 kez tekrarlanmış ve adsorpsiyon

kapasitesinde önemli bir değişiklik gözlenmemiştir. NP'lerin seçiciliği, moleküler yapı, şekil ve boyut açısından Ang II'ye benzer yarışmacı moleküller olan Anjiyotensin I (Ang I) ve Vasopressin (Vsp) varlığında değerlendirilmiştir. Sonuçlar, Ang II-MIP_{np}'in Ang II molekülü için yüksek seçicilik ve duyarlılığa sahip olduğunu ve sentezlenen nanomalzemenin tekrar kullanılabilir olduğunu göstermektedir.

Anahtar Kelimeler: Anjiyotensin II, Nanopartiküller, Moleküler baskılanmış polimerler, Renin-Anjiyotensin-Aldosteron sistemi (RAAS).

ABSTRACT

DEVELOPMENT OF ANGIOTENSIN (II) IMPRINTED NANOPARTICLES

Pırıl ARISOY
M.Sc., Department of Bioengineering

Supervisor: Prof. Gözde BAYDEMİR PEŞİNT
June 2023, 74 pages

Angiotensin II (Ang II) is a peptide hormone that causes vasoconstriction and an increase in blood pressure. It is part of the renin-angiotensin system that regulates blood pressure. The role of Ang II on cardiovascular balance is quite large. Due to its relationship with scientifically proven cardiovascular diseases, it is an important biomarker in blood serum for the detection of diseases. Molecularly imprinted polymers (MIPs) are affinity-based polymeric support materials that enable the recognition of a specific target molecule with high selectivity. Molecular imprinting method is a very frequently used reliable technique to quickly and with high selectivity recognize the desired molecule (eg protein, amino acid, peptide, ion, etc.) from a complex environment. Within the scope of this thesis, Ang II imprinted nanoparticles were synthesized by miniemulsion polymerization reaction for the determination of Ang II from aqueous solutions. For the preparation of hydroxyethyl methacrylate (HEMA) based nanoparticles (NPs), a binary phase mixture was prepared. After Ang II imprinted (Ang II-MIP_{np}) and non-imprinted nanoparticles (NIP_{np}) were synthesized, they were characterized by Zeta Size analysis, Scanning Electron microscopy (SEM), Transmission Electron Microscopy (TEM) and FTIR-ATR spectrophotometer. Specific surface areas were then calculated. The average particle size of the NPs was recorded as 50 nm. The specific surface areas of Ang II-MIP_{np} and NIP_{np} were calculated as 26903.4 and 25868.9 m^2/g, respectively. Ang II molecules were successfully removed from the polymeric structure with a 98% success rate using 0.5 M NaCl solution to obtain template-specific cavities in Ang II-MIP_{np}. Then, the adsorption of Ang II molecules from their aqueous solutions was investigated in terms of their binding capacity to the recognition sites. It has been found that the Ang II adsorption of NPs can go down to 50 pg/mL sensitively. 0.5 M NaCl solution was used for desorption and 98% recovery was

achieved. The adsorption-desorption cycle was repeated 10 times and no significant change was observed in the adsorption capacity. The selectivity of NPs was evaluated in the presence of Angiotensin I (Ang I) and Vasopressin (Vsp), which are competitive molecules similar to Ang II in terms of molecular structure, shape and size. The results show that Ang II-MIP_{np} have high selectivity and sensitivity for Ang II molecule and shows that the synthesized nanomaterial is reusable.

Keywords: Angiotensin II, Nanoparticles, Molecular imprinted polymers, Renin-Angiotensin-Aldosterone system (RAAS).

Dedication

This thesis dedicated to my beloved family, who always loving and supporting me.

ACKNOWLEDGEMENTS

I would like to express my sincere thanks to my esteemed supervisor Prof. Gözde BAYDEMİR PEŞİNT, who has always guided me and provided her endless support with her experience and understanding throughout my graduate education and thesis work.

I would like to thank my dear colleagues Okan ZENGER, Burcu EREN YÜNGEVİŞ, İpek CANATAR and Kardelen CEMEK who have never spared their help and support during my thesis work, and who have made every challenge easier for me with their endless understanding and patience.

I would also like to thank my dear mother and father Neşe ARISOY and Fatih Mehmet ARISOY and my brother Salih Sadi ARISOY for their valuable support and understanding throughout my thesis studies and who have always stood by me under all circumstances.

I would like to thank my friends, especially Şule YÜCE, İrem ACET and Seda DEVRANLI for the encouragement and motivation. They were always there to support me throughout this process.

This thesis was financially supported by ATU BAP Coordination Unit with project number of 22103004.

TABLE OF CONTENTS

LIST OF FIGURES

LIST OF TABLES

LIST OF ABBREVIATIONS

MIP : Molecularly Imprinted Polymer

MIT: Molecular Imprinting Technology

NaCl : Sodium Chloride

Ultrapure water : UPW

HPLC : High-performance liquid chromatography

MS: Mass Spectrometry

FTIR : Fourier transform infrared spectroscopy

SEM : Scanning electron microscope

PBS : Phosphate - buffered saline

EGDMA: Ethylene Glycol Dimethacrylate

PVA: Poly(Vinyl Alcohol)

APS : Ammonium persulfate

SDS: Sodium Dodecyl Sulfate

VIM : 1-Vinylimidazole

HEMA : 2-Hydroxyethylmethacrylate

p(HEMA) : Poly(2-Hydroxyethylmethacrylate)

NP : Nanoparticle

RAAS: Renin-Angiotensin-Aldosterone system

AT1: Ang II type 1 receptor

ACE: Angiotensin Converting Enzyme

Ang II: Angiotensin II

Ang I: Angiotensin I

Vsp: Vasopressin

Ang II-MIP_{np}: Ang II Imprinted Nanoparticle

NIP_{np}: Non-imprinted Nanoparticle

UV : Ultraviolet

LIST OF SYMBOLS

μL : Microliter

μm : Micrometer

nm: Nanometer

mL : Milliliter

mg : Milligram

ng: Nanogram

pg: Picogram

cm : Centimeter

L : Liter

T: Temperature

sec : Second

min : Minute

h : Hour

eq. : Equation

M : Molarity

°C : Celsius degree

CO_2: Carbon Dioxide

k : Selectivity coefficient

k' : Relative selectivity coefficient

IF : Imprinting Factor

1. INTRODUCTION

In human evolution, the Renin-Angiotensin-Aldosterone system (RAAS) played an important role, given its ability to control the salt intake and stimulate thirst. Angiotensin II (Ang II), the central product of RAAS, plays a role in the etiology of hypertension and the pathophysiology of heart and kidney diseases in humans (Yılmaz and Erdem, 2006). Ang II's functions include immune response, inflammation, cell growth and proliferation, largely mediated by the Ang II type 1 receptor (AT1). The primary effector molecule of RAAS is Ang II. It affects the renal tubules to retain salt and water and raises blood pressure in the body (Unger, 2000). It encourages the adrenal gland to produce aldosterone. Ang II is a strong vasoconstrictor but also has proliferative, inflammatory, and fibrotic properties (Benigni et al., 2010). Renin and the enzyme angiotensin converting enzyme (ACE) sequentially cleave the substrate angiotensinogen to generate Ang II, an octapeptide. In particular, Renin breaks down Angiotensinogen to create Angiotensin I (Ang I), which ACE then transforms into Ang II. While the liver produces the Angiotensinogen substrate, the kidney produces renin, and the vascular tissue produces Ang II (Brewster and Perazella, 2004; Fleming, 2006).

Roles of RAAS; blood pressure control has expanded over time far beyond aldosterone synthesis and body fluid and electrolyte homeostasis. Indeed, new actions and underlying signaling mechanisms are continually being uncovered for each member of the RAAS in physiology and disease (Rosenbaugh et al., 2013). However, RAAS research has been going on for over a century. Extended RAAS research; It is believed to be crucial for studies on the heart, kidneys, and hypertension. A variety of regulatory elements and effector peptides make up the RAAS, which facilitates dynamic modulation of vascular function in both health and illness. Clinical therapies that target RAAS and its pathogenic activities have historically placed a crucial emphasis on ACE and Ang II. But new research has also demonstrated the significance of Ang II in preserving RAAS equilibrium (Tikellis and Thomas, 2012).

Renin is an enzyme produced by the kidneys that acts on the precursor molecule Angiotensinogen to produce Ang I. Ang I is then converted by the enzyme ACE to Ang II. Ang II, is a potent vasoconstrictor, it constricts blood vessels, raising blood pressure. Additionally, Ang II stimulates the release of aldosterone from the adrenal glands, which in turn increases the reabsorption of salt and water by the kidneys, further contributing to the increase in blood pressure. Aldosterone is a hormone that regulates electrolyte balance and water balance by increasing the reabsorption of sodium ions and water in the kidneys, and increasing the

excretion of potassium ions. The increased reabsorption of water causes an increase in blood volume, which in turn raises blood pressure. In summary, the RAAS is a series of hormonal interactions that starts with the release of renin by the kidneys, leading to the production of Ang II, which then causes an increase in blood pressure via vasoconstriction and the release of aldosterone which increases reabsorption of water and salt by the kidney leading to an increase in blood volume. Therefore, Ang II is a crucial biomarker for hypertension as well as some conditions linked to hypotension, such as heart attacks, COVID-19, the H1N1 virus, flu infections, malignancies, etc. (Gheblawi et al., 2020). However, Ang II is extremely difficult to detect because it is present in blood at too low amounts and is unstable because of its reactivity. A specific radioimmunological test for Ang II showed its normal concentration in arterial blood to be 2.4 ± 1.2 (S.D.) mμg/100 mL; the venous level is constantly below this value and usually accounts for 50-75% of it (Catt et al., 1969).

Nanoparticles (NPs) are nanoscale materials with dimensions less than 100 nm. They are distinguished from bulk materials by exhibiting a remarkably large surface area/volume ratio and unique optical, electrochemical and thermal properties. As a result of these advantageous features of NPs; It has many common uses such as chemistry, biotechnology, agriculture, communication, defense, electronics, energy, environmental remediation, heavy industries, materials science, medicine, microbiology, optics, and various engineering fields (Mondal et al., 2020).

Polymeric NPs are solid colloidal particles in the size range of 10 nm–1 to μm. NPs, are usually made from biodegradable and biocompatible polymers due to their small size, water solubility, non-toxicity, high shelf life and excellent stability, they can be used in chemical and biological sensing, gas sensing, CO2 capture, purification, drug delivery and targeting, and other related applications (Pillai, 2019).

Molecular Imprinting is a technique used to design artificial biomimetic receptors for a particular analyte (Spieker et al., 2016). Molecularly imprinted polymers are significantly stable polymers that having recognition sites tailored to the three-dimensional form and functionalities of a targeted analyte. These molecularly imprinted polymers can be produced in a covalent or non-covalent fashion (Ensing et al., 2002). Recent studies have shown that molecularly imprinted structures can be used as recognition elements in immunological analyzes by mimicking natural antibodies. Due to their high selectivity and sensitivity, long-term stability and chemical inertness, these artificial recognition elements are applied in clinical diagnostic analysis, as well as for the development of environmental remediation, biotechnological

processes or precursor drug delivery systems. studies are increasing gradually (Baseğmez 2020, Rahtuvanoğlu, 2020; Ergün, 2017, Vasapollo et al. 2011; Lorenzo et al. 2011). The method is fast and inexpensive, and the imprinted polymers are stable enough to be reused (Baydemir G. 2017). Existing hypotheses and models can be tested quickly (Vlatakis et al. 1993).

Although there are several studies in the literature using molecular imprinting techniques for the detection of Angiotensin II molecule, a study that can detect Ang II molecule using NPs has not been reported yet. Therefore, with this thesis study, for the first time, diseases related to hypertension and hypotension, especially heart attack, flu, COVID-19, tumors, etc. The use of Ang II imprinted NPs for illness diagnosis, monitoring, and therapy has been proposed.

This study included the synthesis of Ang II imprinted NPs, characterization of NPs, assays for Ang II selectivity of NPs in the presence of Ang I and Vasopressin (Vsp), competitive molecules that are structurally and formally similar to Ang II, and extraction of Ang II from human blood serum samples.

2. THEORETICAL FOUNDATIONS AND LITERATURE REVIEW

2.1. Renin-Angiotensin-Aldosterone System (RAAS)

When the history of the RAAS is investigated, it emerges that Tiegerstedt and Bergman discovered that raw saline kidney extracts included a toxic chemical they named renin for the first time in 1898 (Atlas et al.,2007). Pathologist Harry Goldblatt and his associates established in 1934 that renal artery restriction led to animals developing chronic hypertension. In 1940, Braun-Mendez and his associates in Argentina and Page and Helmer in the United States discovered that renin was an enzyme that operated on a plasma protein substrate to catalyze the production of the real pressor material, a peptide, which was termed hypertension by the former group and angiotonin by the latter(Atlas et al.,2007).

In order to regulate blood pressure, a series of chemical processes known as RAAS is employed (Colafella et al., 2019; Bader, 2010). When blood pressure falls (for systolic, to 100 mmHg or below), the kidneys release an enzyme called renin into the bloodstream. Renin breaks apart the large protein angiotensinogen, which circulates in the blood. One element is Ang I. The comparably biologically inactive Ang I is broken down by ACE (Bader, 2010). The highly active hormone Ang II is one component. Ang II causes the muscular walls of small arteries (arterioles) to contract, increasing blood pressure (Ames et al., 2019; Bader, 2010). In response to Ang II, the adrenal glands release the hormone aldosterone and the antidiuretic hormone vasopressin (Colafella et al., 2019). When vasopressin and aldosterone are present, the kidneys retain sodium (salt). Aldosterone also encourages potassium excretion by the kidneys. High salt levels cause water retention, increasing blood volume and blood pressure (Colafella et al., 2019; Ames et al., 2019). New actions and underlying signaling mechanisms are continually being uncovered for each member of the RAAS in physiology and disease (Rosenbaugh et al., 2013). However, research into a RAAS has been going on for over a century. Extended RAAS research; It is thought to play an important role in cardiovascular, renal, and hypertension research. A variety of regulatory elements and effector peptides make up the RAAS, which facilitates dynamic modulation of vascular function in both health and disease.

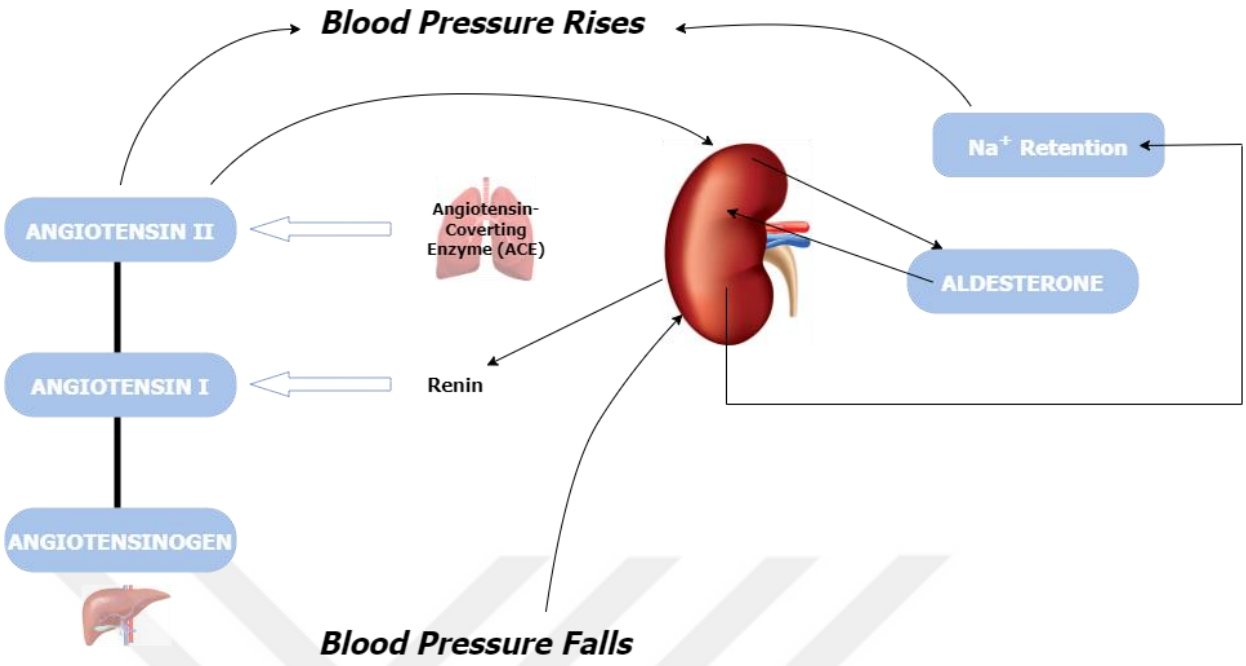

Figure 2.1. The basic working principle of the RAAS

2.2. Introduction to Angiotensin II

Ang II is a peptide-based hormone that included 8 amino acids. It's a small component compared to Ang I and Angiotensinogen. Ang II; is one of the five basic components that make up the RAAS; It plays a role in the etiology of hypertension and the pathophysiology of heart and kidney diseases in humans (Fyhrquist et al., 2008; Yilmaz and Erdem, 2006). Ang II's functions include immune response, inflammation, cell growth, and proliferation, largely mediated by the Ang II type 1 receptor (AT1). Two main G-protein-coupled receptors transmit the actions of Ang II with seven-transmembrane domains, AT1 and AT2. However, most cardiovascular effects of Ang II are conveyed by the AT1 receptor (Bader et al., 2010). The primary effector molecule of RAAS is Ang II. It affects the renal tubules to retain salt and water and raises blood pressure in the body (Unger, 2000). It encourages the adrenal gland to produce aldosterone. Ang II is a strong vasoconstrictor but also has proliferative, inflammatory, and fibrotic properties (Benigni et al., 2010). Angiotensinogen is converted into Ang II, an octapeptide, by the successive action of the enzymes renin and ACE. Specifically, Renin breaks down Angiotensinogen to create Ang 1, which ACE then turns into Ang II. While the liver produces the Angiotensinogen substrate, the kidney produces renin, and the vascular tissue produces Ang II (Brewster and Perazella, 2004; Fleming, 2006).

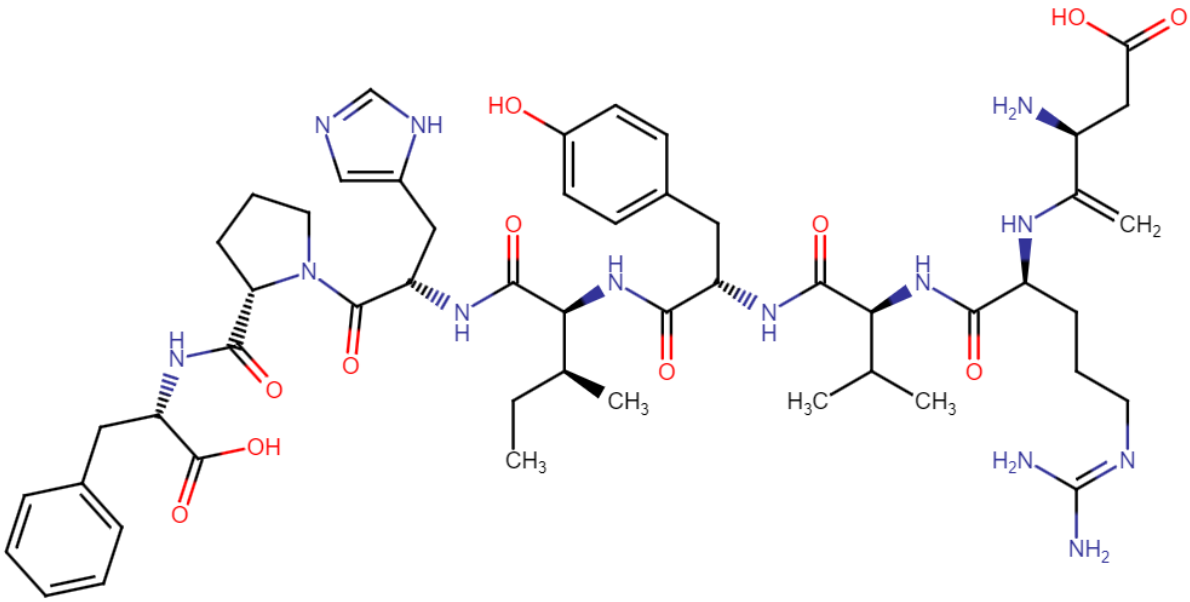

Figure 2.2. Chemical Structure of Angiotensin II

In recent years, therapeutic therapies that target RAAS and its pathogenic activities have mostly concentrated on ACE and Ang II. However, new research has also shown the significance of Ang II in preserving RAAS harmony (Tikellis and Thomas, 2012). Vasoconstriction, aldosterone release, the production of antidiuretic hormone, sympathetic activity, and salt absorption from the renal tubules are Ang II's actions in the body. However, all of these effects may result in the onset of hypertension if the RAAS system is dysfunctional. The direct contractile impact of Ang II on arterial smooth muscles is the most significant effect in hypertension. Along with causing atherosclerosis, heart muscle myositis development, left ventricular hypertrophy, and heart failure, it also results in abnormalities in endothelial cells, medial hypertrophy, and an increase in connective tissue (Chappell, 2016). Additionally, recent research has demonstrated that the Severe Acute Syndrome Coronavirus-2 (SARS-CoV-2) causes elevated Ang II levels that cause ACE 2 to be down-regulated. As a result, Ang II is a crucial biomarker for hypertension and several conditions linked to hypotension, such as heart attack, COVID-19, H1N1 influenza, flu infections, malignancies, etc. (Ghebhawi et al., 2020). However, Ang II is extremely difficult to detect since it is present in the blood in very low amounts and is unstable because of its reactivity.

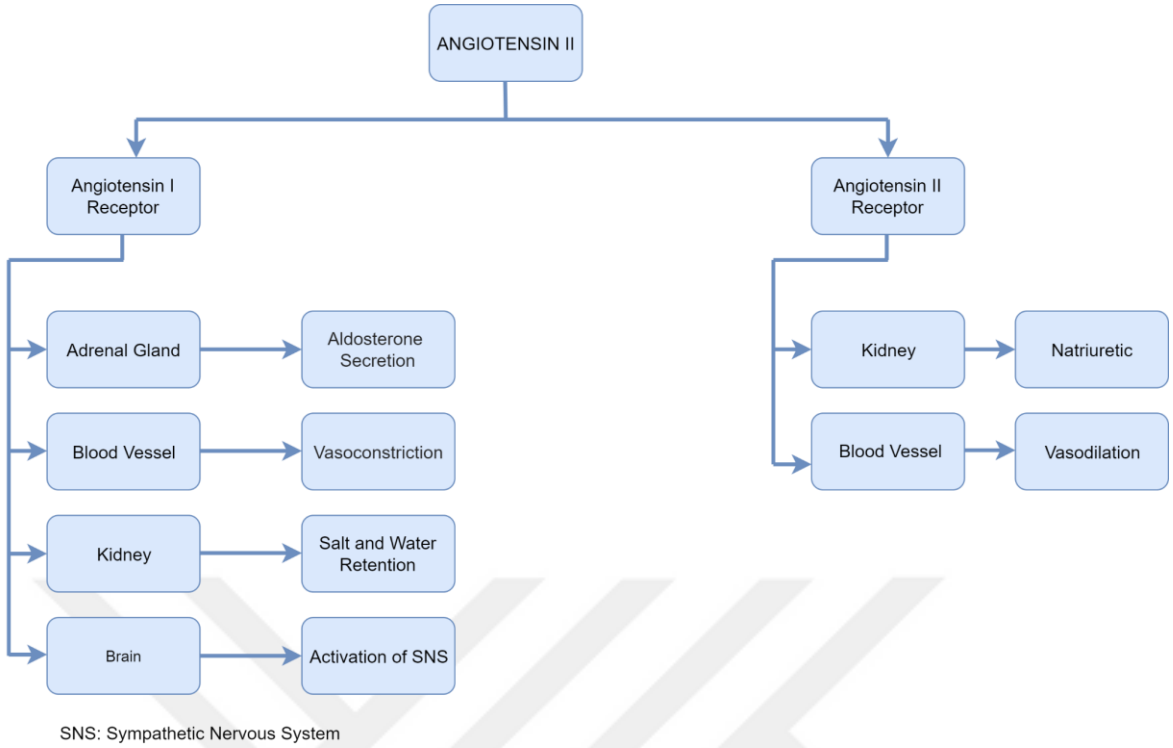

Figure 2.3. Diagrammatic Representation of Angiotensin Receptors

A specific radioimmunological test for Ang II is 2.4 ± 1.2 (SD) mμg / 100 mL of its normal concentration in arterial blood has shown that; the venous level is constantly below this value and usually accounts for 50-75% of it (Catt et al., 1969). HPLC radioimmunoassay (RIA) is the most used technique for detecting angiotensin and its metabolites in bodily fluids (Voelker et al., 1994). Although this procedure necessitates the management and disposal of radioactive waste, it is rather drawn out and difficult. Alternative methods are being investigated for the detection of angiotensin peptides in blood as a result of these factors. At 210 nm, angiotensin is detectable by UV, however this method is not highly sensitive or specific. Additionally, after pre- or post-column derivatization of the terminal amine group with an electroactive or fluorescent label, fluorescence detection and electrochemical (EC) detection were employed (Kobori et al., 2008; Gosetti et al., 2010). Wider usage of mass spectrometry (MS) for the identification of peptides by LC and CE has recently occurred. However, this detection method's application has been constrained due to the total expense of implementation and issues that might occur while analyzing biological fluids (Danser, 2003).

2.3. Nanotechnology

The concept of nanotechnology, in terms of its etymological roots, consists of the combination of the Greek word "nano" meaning "dwarf" and the concept of "technology". The nanostructures are approximately 1-100 nm in length corresponds to systems (Milunovich et al., 2004). To put it in concrete terms; On average, it is approximately 10000 times smaller than human hair. When the size of the material is reduced to nanometers, its physical properties begin to change, that is, different properties begin to be observed compared to normal systems (Doğan, 2005; Ciraci et al., 2005). Nanotechnology; It is the understanding and control of physical, chemical and biological phenomena at the nanometer scale, and the development and production of functional materials, tools and systems at these dimensions (Ciraci et al., 2005).

In 1959, physicist Richard Feynman made an effort to draw the attention of scientists to nanometer dimensions by emphasizing this aspect of nanostructures, with his famous speech on the possibility of producing materials and devices at molecular dimensions (Ciraci et al., 2005). Thus, in the last quarter of the 20th century, the era of designing and synthesizing new nanostructures that are not found in nature at the atomic level has begun. As Feynman predicted in his speech in 1959, which is accepted as the milestone of rapidly developing nanotechnology, small-scale studies are increasing and developing day by day. The control of materials and structures at the nanoscale can be possible with engineering approaches (Wu et al., 2021; Bayda et al., 2019). It is possible to obtain very light, high-strength, smart, very cheap, clean materials with nanotechnological studies, which offer a completely different and new perspective to biology and medicine research (Hu and Niemeyer, 2019; Wu et al., 2021; Goldberg, 2019; Weiss et al., 2020; Ernst et al., 2019). It has been revealed that nanomaterial studies can be directed to the desired place according to many different purposes in the industry and in our lives (Goodsell, 2004).

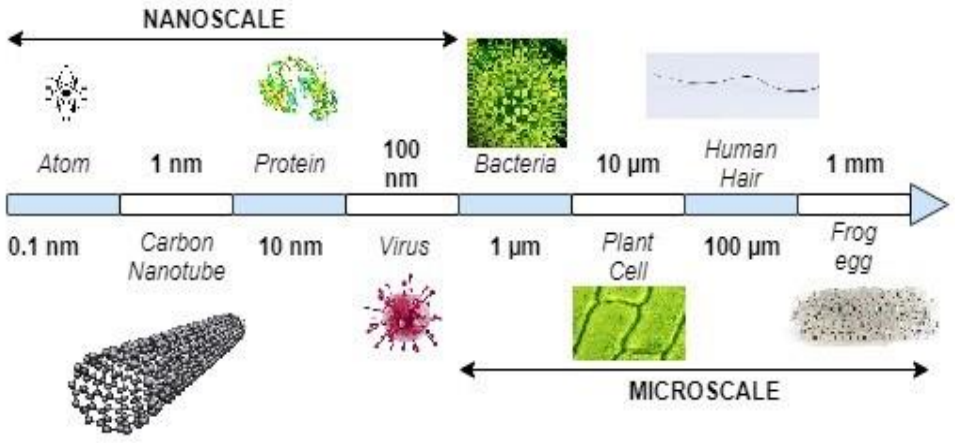

Figure 2.4. Nanoscale and Microscale

As researchers began to work in smaller sizes, many problems began to emerge. The basis of nanotechnology applications is based on the change of physical properties as a result of the reduction of material sizes. For example, NPs have a very large surface area to volume ratio. Accordingly, optical properties such as fluorescence become a function of particle diameter. Hardness and elasticity properties change in materials made using NPs. It is possible to strengthen conventional polymer structures using NPs. While the weight of such nanotechnologically reinforced materials decreases, durability and functional diversity increase. However, as the dimensions shrank, it became more challenging to keep track of the job being done. The scanning tunneling microscope (STM), a brand-new kind of microscope, was created by IBM in 1981, and the researchers behind it were given the Nobel Prize in Physics in 1986. The "atomic force microscope" (AFM), a variation of the STM microscope that is currently often employed in describing nanomaterials investigations, was also created at the same time. With the development of computer capacities in the 1980s, measurement and modeling at the nanometer scale became possible. In the early 1990s, researchers at Rice University led by Richard Smalley developed soccer ball-shaped "fullerene" molecules, made by a symmetrical arrangement of 60 carbon atoms. The resultant molecule had a size of one nanometer, was lighter and stronger than plastic and steel, and could transport heat and electricity. The 1996 Nobel Prize in Chemistry was given to these scientists. Carbon nanotubes were discovered in 1991 by Sumio Iijima, a researcher of the Japanese NEC corporation. A stretched version of the fullerene molecule, carbon nanotubes exhibited essential qualities that were comparable to those of steel, including being 100 times stronger and weighing just 1/6 as

much. Eric Drexler's book (Engines of Creation), which was published in the 1990s, expanded on Feynman's theories. Drexler's theories received criticism, but he went into great detail with his broad notions and ideas in his book, Nanosystems: Molecular Machinery, Manufacturing, and Computation, released in 1992. The National Nanotechnology Initiative, the first official government initiative in the United States under Bill Clinton, was introduced in 1999 with the goal of accelerating the activities of research, development, and commercialization in the nanotechnology sector. Nanotechnology studies were added as a priority topic in the Framework Program by the European Union in 2001. If we count the countries where the most literature on nanotechnology is produced; firstly Japan, followed by America, Germany, Canada and France. However, in recent years, studies and investments for nanotechnology research in our country have started to increase significantly with government incentives (Çalık et al., 2021; Nanoteknoloji Strateji Grubu, 2023). It has been included in the Vision 2023 Program prepared by TÜBİTAK as one of the priority areas. In the 9th Development Plan, it was stated that areas such as biotechnology and nanotechnology came to the fore in terms of developed countries, and these areas were shown first among the priority areas to be supported. It is stated that nanotechnology-related projects will be given priority in the research projects to be supported by the State Planning Organization (Nanoteknoloji Strateji Grubu, 2023). A nanotechnology research center (UNAM) was established at Bilkent University with the support of TÜBİTAK. Currently, nanotechnological studies are carried out in various fields of science in many universities.

2.4. Nanobiotechnology

Contemporary science; in order to examine biological events at the molecular level, it tries to understand especially very fast and many parallel and/or consecutive biological reactions and to provide technological developments in order to increase the quality of life in the light of these reactions (Çorman, 2010). The definition of the concept of nanobiotechnology was found with the development of a topic that emerged during these studies. The sub-branch of nanotechnology that includes biological and biochemical applications is called nanobiotechnology. In recent years, great developments in molecular biology and gene technology, both in the world and in our country, have been the driving force of rapid change and progress in nanobiotechnology, and this technology covers and affects more and more industries and service sectors.

The most important opportunity offered by nanotechnology for biology is to create new tools for the investigation of biomolecular structure, function and properties (Morais et al., 2014; Yaqoob et al., 2020; Çorman, 2010). When these new tools are used, it is possible to directly measure the structural elements and molecular relationships of the cell. In the development of nanobiotechnology, the construction of nano-sized devices by imitating biological mechanisms plays an important role.

Nanobiotechnology; creates extraordinary models to emulate and then provides us with ready-to-work components that will combine synthetic and biological nanotechnology to create hybrid structures (Morais et al., 2014; Yaqoob et al., 2020; Çorman, 2010). Many areas of life such as human health, agriculture, chemical engineering, environmental protection, food production, and energy production are within the scope of this technology. Nanobiotechnology is an interdisciplinary science that includes technologies used for the diagnosis, follow-up and treatment of many diseases, biosensing, biological separation, molecular imaging, anticancer treatment and development of plants and animals, with the help of the working mechanisms of living organisms and biological structures (Brown et al., 2010; Morais et al., 2014; Yaqoob et al., 2020; He et al., 2019; Bayda et al., 2019). It includes the development of products for the improvement of living things and their quality of life or their industrial use, and the application of modern technology to natural sciences (Çorman, 2010).

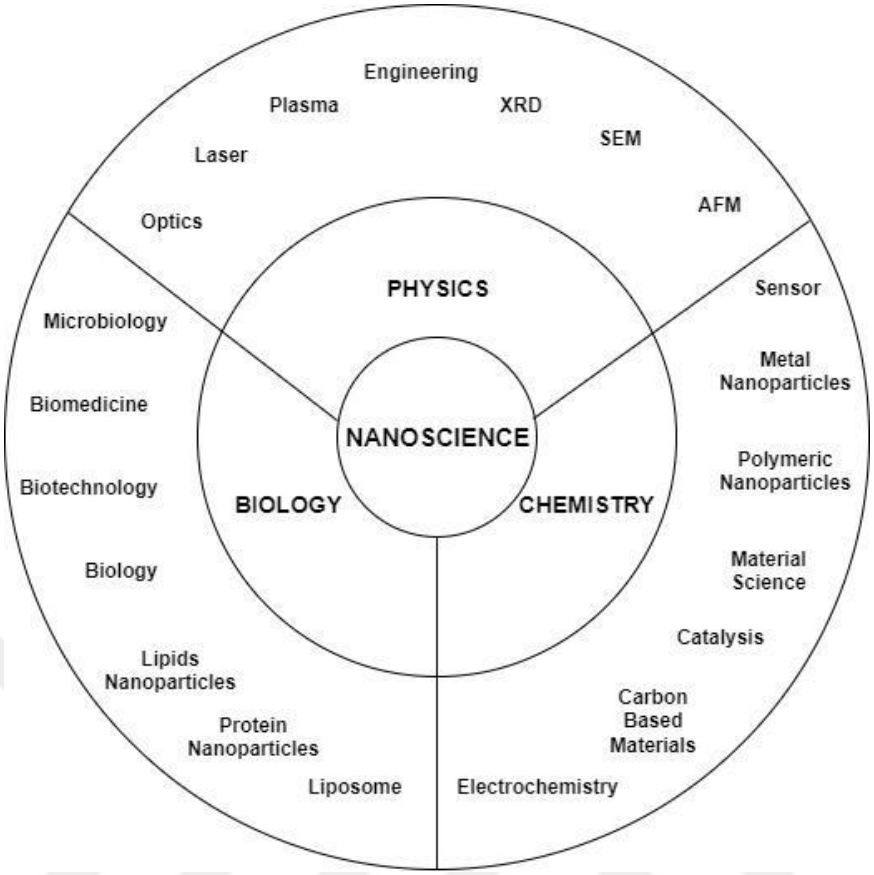

Figure 2.5. Applications of Nanotechnology

2.5. Nanoparticles

NPs, which can also be called nanospheres and nanocapsules; are defined as nanoscale materials with dimensions less than 100 nm. They differ from bulk materials in that they exhibit unique optical, electrochemical and thermal properties with a significantly large surface area/volume ratio. As a result of these unique features; It has widespread usage areas such as chemistry, biotechnology, agriculture, communication, defense, electronics, energy, environmental remediation, heavy industries, materials science, medicine, microbiology, optics and various engineering fields (Mondal et al., 2020).

In the nanosphere, the active substance is homogeneously dispersed in the matrix system. In the nanocapsule, the active substance is surrounded by a polymeric membrane. The desired properties of NPs can be listed as controlled release of the drug, degradation of the carrier in the physiological environment, and non-toxicity of the degradation products (Mitchell et al., 2021; Salata, 2004). Monosized NPs are suitable for biolabeling applications. Biolabeling, biological or molecular coating should be based on layer-forming NPs with a bioinorganic

surface. Biological coating; It contains antibodies, biopolymers such as collagen and monolayers of small molecules (Salata, 2004).

NPs, which form the starting point of nanotechnological materials, can be produced in a wide chemical range and morphology (Gürmen and Ebin 2008). NPs, which are defined as powders with dimensions of 100 nm and below, form the basis of nano-sized materials, thus nanotechnology (Khan et al., 2019; Miller et al., 2004; Rao et al., 2005). These particles show properties that are generally considered different and superior to other commercial materials. It is clear that the production of NPs is an indispensable first step for new developments in nanotechnology, which includes the design, production and functional use of nanostructured materials and devices.

Generally, there are three layers that make up the NPs (Mitchell et al., 2021; Khan et al., 2019). These are;

- The surface layer that can be functionalized with various small molecules, metal ions, surfactants and polymers;
- The crustal layer, which is a material that is chemically different from the core in every way;
- The core, which is the central part of the NP.

NPs can also be used in drug delivery, chemical and biological sensing, gas sensing, CO2 capture and other related applications (Mitchell et al., 2021; Salata, 2004; Khan et al., 2019; Li et al., 2022).

Studies conducted in recent years show that the most important parameter for NP drug delivery systems or bioconjugants to reach the target cell and to be taken into the cell by endocytic means is to remain in circulation for a time that allows the carrier system to interact with the target. For this reason, ligand-receptor-mediated targeting comes to the fore by using steric stabilization and targeting ligands together in drug delivery system design, which increases the residence time in biological fluids or circulation and prevents interaction with opsonizing components (Mitchell et al., 2021; Salata, 2004).

NPs, which can be classified according to features such as specific shape, size, activity and the type of materials from which they are made, generally consist of two groups as inorganic and organic particles (Sajid and Płotka-Wasylka, 2020). Inorganic NPs are produced by precipitation of inorganic salts that bind to molecules by metallic and covalent interactions.

Synthetic and natural organic compounds such as milk emulsion, protein aggregates, lipid bodies and other complex structures are used to produce organic NPs (Sircar et al., 2022).

Inorganic NPs;

- Carbon-based NPs
- Metal and metal oxide NPs
- Semiconductor NPs
- Ceramic NPs

Organic NPs;

- Polymeric NPs
- Biomolecule derived NPs (Sajid and Płotka-Wasylka, 2020).

Polymeric NPs are solid colloidal particles in the size range of 10 nm^{-1} to μm. Generally, NPs made from biodegradable and biocompatible polymers are used as drug carriers by encapsulating drugs, in chemical and biological sensing, gas sensing, CO_2 capture, purification and other related applications due to their small size, water solubility, non-toxicity, high shelf life and excellent stability (Pillai, 2019).

2.5.1. Synthesis methods of nanoparticles

Physical, chemical, and biological processes are used to create NPs, and these processes may be roughly categorized into bottom-up and top-down techniques (Dhand et al., 2015; Ramanathan et al., 2021). The synthesis conditions dictate the fundamental characteristics of NPs. These characteristics include, but are not limited to, size and size distribution, crystallinity, form, and directional qualities (Sajid and Płotka-Wasylka, 2020).

(a) Bottom-up approach; by mixing atoms, molecules, or tiny particles, NP synthesis employs the bottom-up strategy and depends on the production of NPs from small molecules. This approach involves first creating the NP building components, which are then joined to create the final NP. (Khan et al., 2019; Dhand et al., 2015; Ramanathan et al., 2021).

(b) The top-down approach involves reducing bulk materials to nano-sized particles. The size reduction of the initial material through various physical and chemical processes is the basis for the production of NPs (Khan et al., 2019; Dhand et al., 2015; Ramanathan et al., 2021). It uses techniques including thermal, laser, and mechanical milling. Top-down approaches are simple to use, but they are unsuitable for creating particles with

irregular shapes and very low sizes. The primary issue with this technique is the alteration of NPs' physicochemical and surface chemistry (Nadagouda et al., 2011).

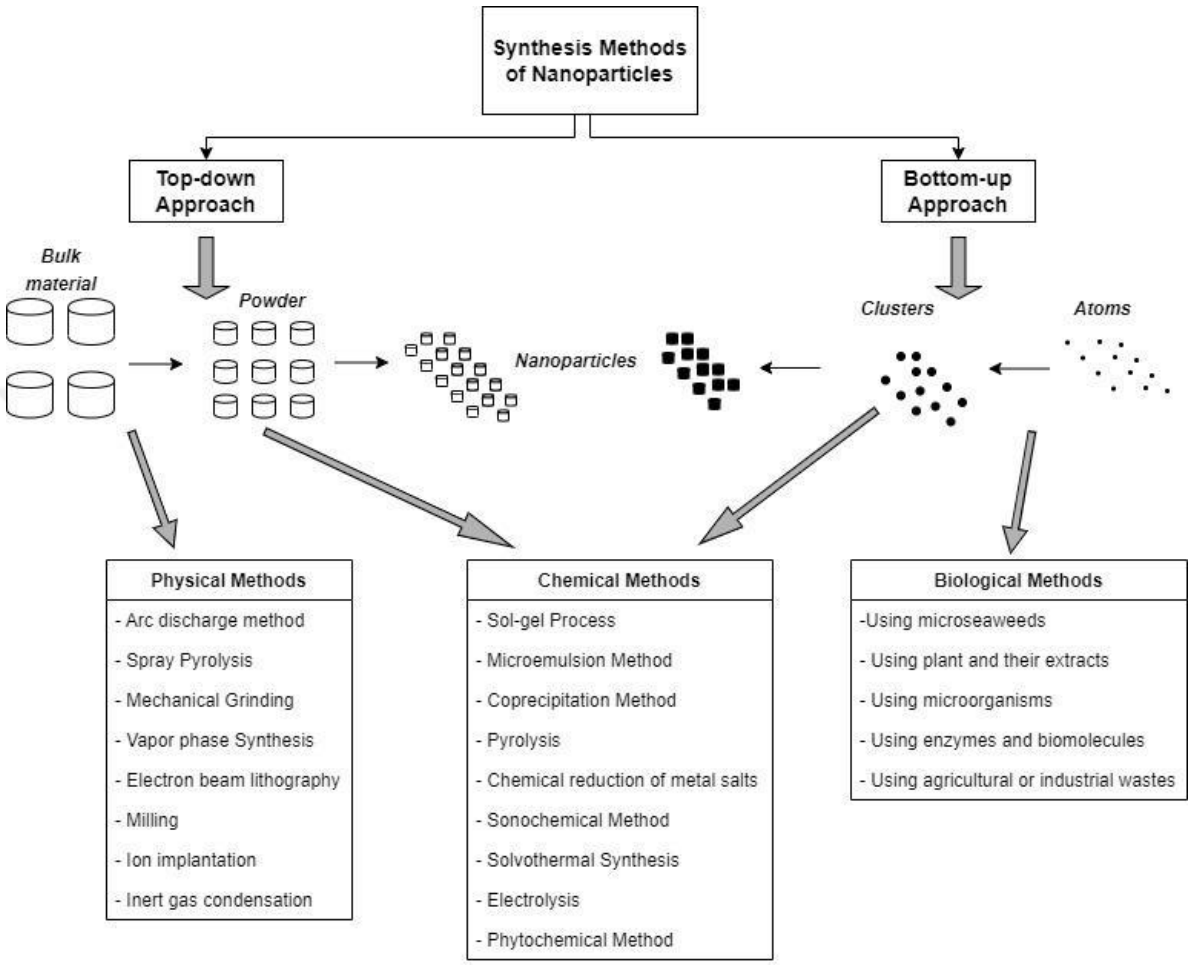

Figure 2.6. Synthesis methods of NPs (Khan et al., 2019; Dhand et al., 2015)

2.6. Molecular Imprinting Technology

The selective identification of molecules is used to achieve many fundamental biological interactions in nature. It is extremely difficult to create artificial affinity receptors that can replicate such activities. Recent advancements in molecular imprinting technology have made it a crucial technique for creating synthetic receptors because to its benefits, including robust recognition and straightforward mass manufacturing. (Mahony et al., 2005; Taguchi et al., 2015). Due to its distinctive characteristics of structural predictability, recognition specificity,

and application universality, molecular imprinting technology has been extensively used in a variety of industries.

A methodology for creating molecularly imprinted polymers (MIPs) with specially manufactured binding sites that are complementary to the template molecules in terms of form, size, and functional groups is known as molecular imprinting technology (MIT) (Chen et al., 2016; Curcio et al., 2009). Pauling's theories about the production of antibodies by the immune system served as an inspiration for the concept of molecular imprinting (Mosbach and Ramström, 1996). According to Pauling's theory, antibodies acted like denatured proteins because they were free of hydrogen bonds and their chains could move about (Bergmann et al., 2007). This hypothesis of Pauling inspired the idea of a freely moving polymer chain that can form a complementary pattern around a structure. In 1966, Mosbach published the immobilization of enzymes and cells trapped in a polyacrylamide gel, mainly through non-covalent interactions, which form the basis of biomolecule imprinting (Mosbach and Mosbach, 1966; Curcio et al., 2009). The imprinting of organic polymers by the covalent approach was first reported by Wulff in 1972 (Wulff, 1972). According to this approach, covalent complex formation was required between the mold and the polymer surrounding the mold. While the typical templates for covalent imprinting are small organic molecules, the non-covalent interaction method has extended the pattern diversity to large biomolecules such as protein, DNA and RNA.

In terms of theory, the molecular imprinting of synthetic polymers involves the co-polymerization of functional and cross-linking monomers in the presence of the target analyte (imprinted molecule), which serves as a molecular template (Haupt and Mosbach, 2000; Taguchi et al., 2015). In the first step, the functional monomers form a complex with the printing molecule and then polymerization occurs. The strongly crosslinked polymeric structure holds its functional groups in place once polymerization has occurred (Chen et al., 2016). Removal of the imprint molecule from the structure by various effects reveals binding sites for the analyte that are complementary in size and shape. In this way, the residue is incorporated into a molecular memory polymer that can rebind the target analyte with very high specificity (Chen et al., 2016; Haupt and Mosbach, 2000). Vasoconstriction, aldosterone release, antidiuretic hormone production, sympathetic activity, and salt absorption from the renal tubules are biological events that are directly affected by the Ang II level in the body.

MIPs are used in many areas such as purification, separation, chemo/bio detection, artificial antibodies, drug release/catalysis and degradation, thanks to their high physical stability (Andaç

et al., 2018; Parisi et al., 2020; Parisi et al., 2022; Li et al., 2009; Wang and von Recum, 2011; Alvarez-Lorenzo and Concheiro, 2004; He et al., 2021).

2.6.1. Fundamentals of Molecular Imprinted Polymers Synthesis

Molecular imprinting takes place in three primary stages:

1. **Self-assembly**

   At this stage, which is also called pre-complexation, the template molecule with selected suitable monomers forms a complex by binding with different interactions (covalent or non-covalent interactions). In the selection of monomers; functional groups and their ability to polymerize play a role. Functional monomers form a new structure by functional reorganization around the template molecule. In the meantime, electrostatic, hydrophobic, Van der Waals or hydrogen bond interactions come into play, and complexations occur depending on the three-dimensional structure and chemical properties of the target molecule (template molecule).

2. **Cross-linking**

   It is the step of selecting suitable crosslinkers and polymerizing the template-monomer pre-complex with crosslinkers.

3. **Extraction**

   In this step, which includes the removal of the template molecule; a washing agent that interacts more with the functional monomer than with the target molecule is used. At the end of this process, cavities are formed on the polymer surface with a specific shape and binding sites for the target molecule. Thus, under suitable conditions, a structure that recognizes the physicochemical characteristics of the template molecule is selective and can bind the template molecule effectively is obtained.

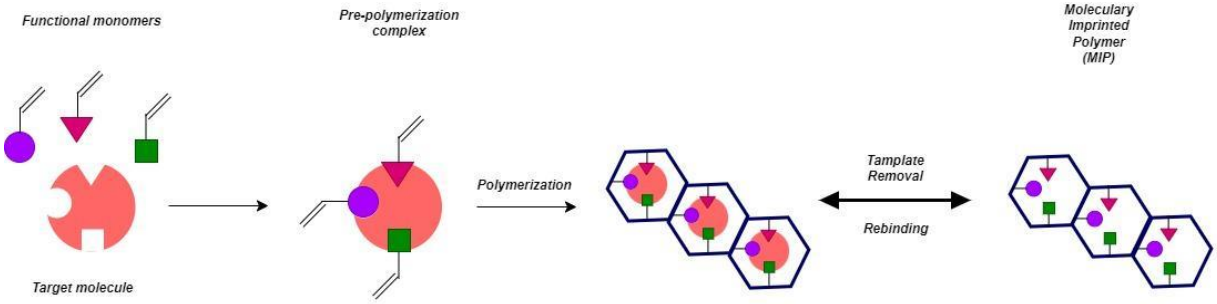

Figure 2.7. General scheme of the MIP process

According to the type of bond between the template molecule and the functional monomer in molecular imprinting; There are three main methods: covalent, non-covalent and semi-covalent imprinting (Chen et al., 2016; Haupt and Mosbach, 2000; Alexander et al., 2006).

Table 2.1. Properties and characteristics of polymers

Properties	**Characteristics**
Physical Resistance	Resistant to mechanical stress, high pressure and high temperature
Chemical Resistance	Resistant to acids, bases, various organic solvents and metal ions
Storage Resistance	It can last for a very long time without losing performance
Capacity	0.1-1 mg imprinted molecule/g polymer
Recyclability	>99%

2.6.2. Imprinted by Covalent Binding

It is a molecular imprinting method in which functional monomers and template molecules form reversible covalent bonds while forming a polymerization pre-complex, and reattachment of the template to the structure after it is removed from the MIP is based on covalent bonds (Curcio et al., 2009). In covalent interactions, there is a certain stoichiometric ratio between the monomer and the template molecule. The covalent bonds formed after polymerization are broken. The same covalent bond is re-formed when the target molecule interacts with the imprinted polymers (Whitcomb et al., 2014; Mosbach and Ramström, 1996).

2.6.3. Imprinted by Non-Covalent Binding

In the non-covalent imprinting method, non-covalent forces such as hydrogen bonds, ionic interactions, hydrophobic interactions and metal chelation interactions are used both during molecular imprinting and re-attachment of the template molecule to the structure (Chen et al., 2016; Whitcomb et al., 2014; Mosbach and Ramström, 1996). Covalent modification of the template molecule is not required and different binding interactions can be used to form the template monomer complex. Non-covalent binding kinetics are similar to enzyme-substrate bindings compared to covalent binding (Sellergren et al., 1988). When the molecular imprinting method was first introduced, covalent bonds were used for polymerization. However, as the method was developed, non-covalent interactions offered more advantages because they were easier to apply, and for this reason, they started to be preferred more.

2.6.4. Imprinted by Semi-Covalent Binding

This method offers a more advantageous approach by combining the advantages of both covalent and non-covalent strategies to control the microenvironment of imprinted polymers (Taguchi et al., 2015; Curcio et al., 2009). In suppression with semi-covalent bonding; It is based on the polymerization of a template covalently linked by a cleavable bond to a functional monomer (Curcio et al., 2009; Tan and Tong, 2007). After copolymerization has taken place, template removal leaves imprint-bearing functional groups that can interact non-covalently with the template in the step of relinking the analyte to the structure (Qi et al., 2010). The semi-covalent approach offers advantages such as the formation of homogeneous binding sites by covalent imprinting and rapid and reversible adsorption with non-covalent imprinting (Tan and Tong, 2007).

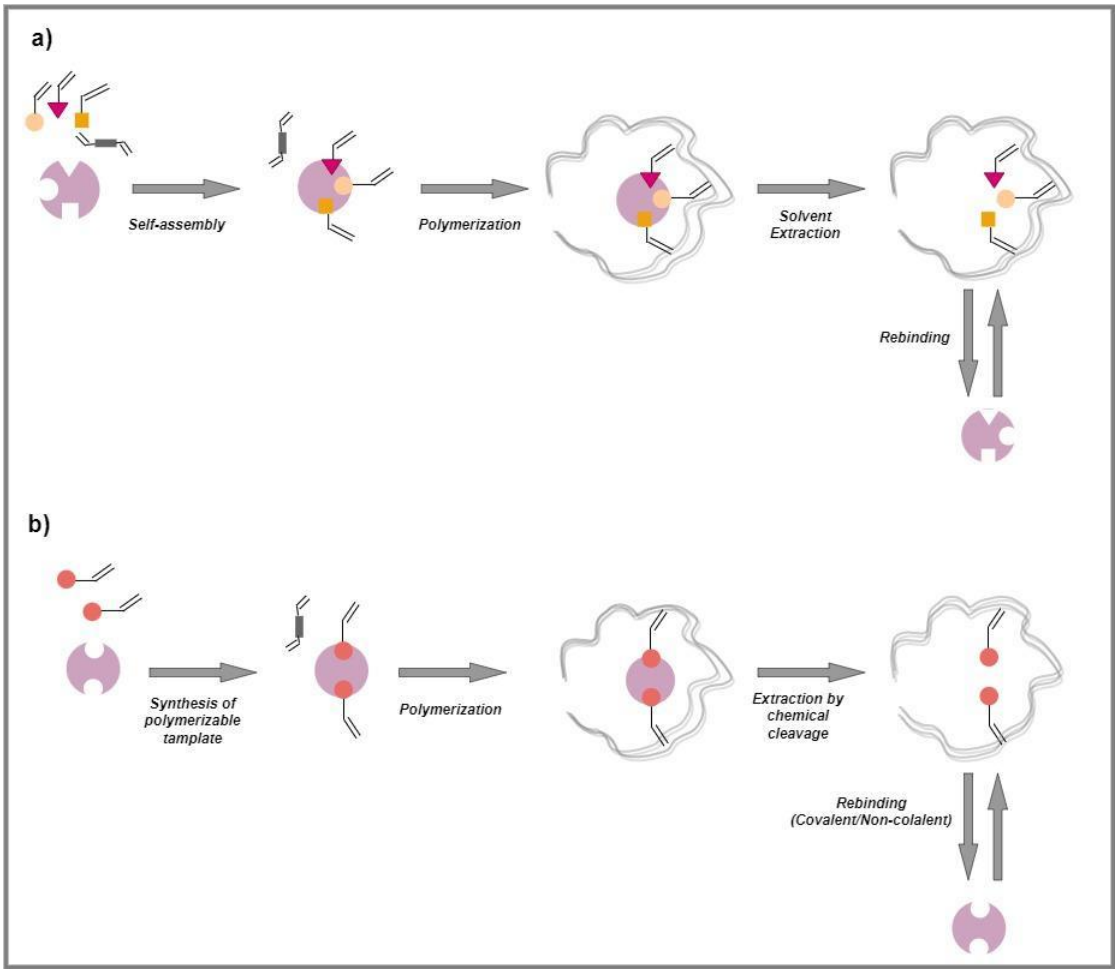

Figure 2.8. Schematic representation of Molecular Imprinting Approaches a) non-covalent, b) covalent /semi-covalent molecular imprinting methods

2.6.5. Components of Molecular Imprinted Polymer Synthesis

2.6.5.1. Template/Target Molecule

In the molecular imprinting method, the structure and properties of the target molecule or ion to be imprinted molecule are critical since will interact with monomers with suitable functional groups. The template molecule to be imprinted contains a group that will polymerize, the presence of a group that will prevent or slows down the reaction, and the stability of the molecule at high temperatures are important parameters. As the number of bonding groups in the target molecule increases, the interacting region also increases. Molecules to be imprinted, which vary according to the purpose of the study; drugs, amino acids, ions, carbohydrates, proteins, hormones, coenzymes, nucleotide bases, and pesticides. (Cormack and Mosbach, 1999).

2.6.5.2. Functional Monomer

The selection of functional monomers is very important for the stability of the functional monomer-template molecule complex during the imprinting process. The most important feature for functional monomer selection is the number of binding sites available for interaction to occur (Gao et al., 2020). It is important to match the functional groups of the functional monomer and the molecule or ion to be imprinted in order to increase the complex formation and imprinting effect. Functional monomers are divided into monomers with acidic, basic and neutral properties.

Table 2.2. The most used functional monomers in the synthesis of MIPs (Scorrano et al., 2011)

Functional Monomer	Structure	Functional Monomer	Structure
Vinyl Benzoic acids	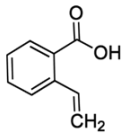	Vinyl pyrimidines	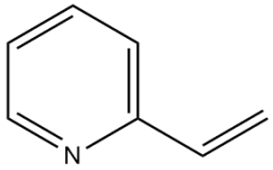
Amino Methacryl Amides	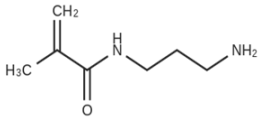	Acrylamide Sulfonic acids	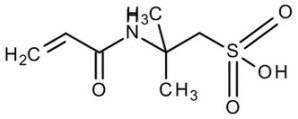
Vinylimidazole	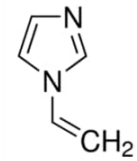	4-(Vinylbenzyl)iminodiacetic acid	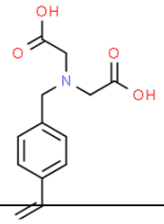
Acrylic acids	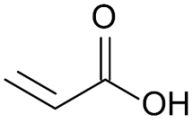	N, N'-Diethyl-4-vinylbenzamine	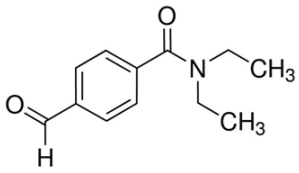

2.6.5.3. Cross-linker

Another important point when preparing MIP is the choice of crosslinker. Crosslinkers; Controlling the morphology of the polymer matrix (either gel type, macroporous or microgel

powder) is responsible for the stability of the imprinted molecule or ion attachment points, and the mechanical stability of the polymer matrix (Idziak et al., 2001). For an effective imprinting process to occur, there must be compatibility between the crosslinkers and the functional monomers (Gao et al., 2020). Otherwise, either one will play a more dominant role during polymerization and copolymerization will not occur. At the same time, stoichiometric balance must exist between the crosslinker and the functional monomer (Biçen, 2010). In very large molar ratios, crosslinkers show non-covalent interactions with functional monomers or the target molecule, reducing the effectiveness of the imprinting . In very small mole ratios, the binding sites of the template molecules come very close to each other. The binding sites of the target molecule are closed by the neighboring regions and an effective result cannot be obtained again (Chapuis et al., 2004). Ethylene glycol dimethacrylate (EDMA) and divinyl benzene (DVB) are commonly used crosslinkers.

Table 2.3. The most used crosslinkers used in preparing molecularly imprinted polymers

Crosslinker	Structure	Crosslinker	Structure
Pentaerythritol triacrylate	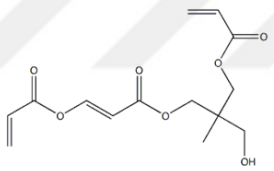	Trimethylolpropane trimethacrylate (TRIM)	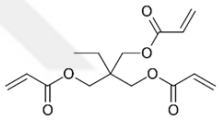
p-Divinylbenzene	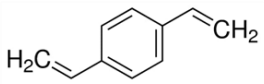	N,N'-1,4-phenylenediacrylamide	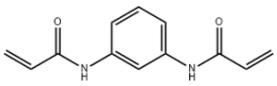
Ethylene glycol dimethacrylate (EDMA)	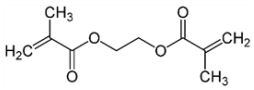	N,O-bisacryloyl-L-phenylalanineol	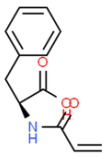
N,N'-Methylene acrylamide	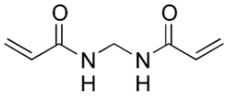	Pentaeritrol tetraakrilat	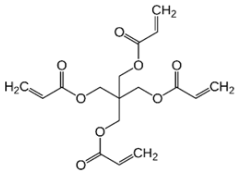

2.6.5.4. Solvent

Generally, MIPs are prepared in solvent-based environments. Therefore, an important point in the synthesis of MIPs is the choice of solvent. Solvents are used selectively, depending on the

type of printing method. In non-covalent imprinting polymerization; It also has the task of increasing the complex formation between the target molecule and the functional monomer (Okay, 2000). At the same time, the choice of solvent is important to increase the formation of non-covalent interaction between the target and the functional monomer and the suppression effect. In addition to the dissolution of the polymerization components, the presence of all components in one phase, the solvent provides pore formation and homogeneous distribution of the temperature. In this way, it prevents the formation of unwanted by-products. Generally, MIPs using non-polar organic solvents for synthesis have better selectivity than MIPs using polar organic solvents (Yu and Mosbach, 1997). The usage of polar solvents reduces the interaction forces that will occur between template molecule and functional monomer, which will reduce the recognition capacity. In addition, MIPs show different swelling properties in different solvents. Swelling; Since it changes the three-dimensional structure of the functional groups and this leads to a change in the selectivity of MIP, weaker bindings occur in the analyte recognition step (Yu and Mosbach, 1997).

2.6.5.5. Initiator

The role of the initiator in radical polymerization is very important, as the initiator is responsible for the formation of monomer radicals to enable polymer formation. Many chemical initiators with different chemical properties are used as radical sources in free radical polymerization. The most commonly used initiators are 2,2-azobis(isobutyronitrile) (AIBN) and 2,2-azobis (2,4-dimethylvaleronitrile) (ADVN) (Turiel et al., 2005; Fu et al., 2003). In cases where the interactions between the monomer and the target molecule are very weak, very high temperatures cannot be reached. Under these conditions, UV degradation is preferred over thermal degradation (Cormack and Elorza, 2004).

Table 2.4. The most used initiators used in preparing molecularly imprinted polymers

Initiator	Structure
Ammonium persulfate	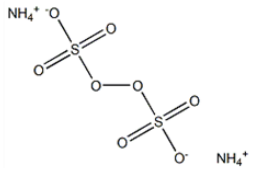
Azobisisobutyronitrile	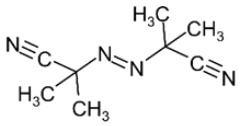
Azobis dimethyl valeronitrile	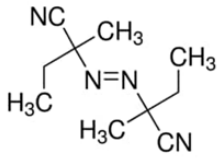
Dimethyl acetal benzyl	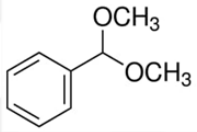
Benzoyl Peroxide	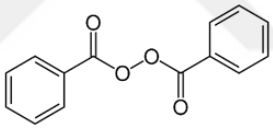
Azo cyanovaleric acid	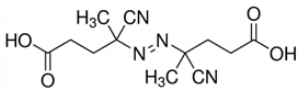

2.7. Polymerization Techniques of MIPs

2.7.1. Bulk Polymerization

In this process; Since the amount of solvent used is so small, it results in bulk material, the term bulk polymerization has been given by the Molecular Imprinting Association (Albericio and Tulla-Puche, 2008). In bulk polymerization; after adding a suitable initiator into the monomer, it can be directly polymerized at a certain temperature and pressure. The bulk polymerization method is quite convenient and easy. It does not require specific skills or advanced equipment (Bitas and Samanidou, 2018) and has proven its effectiveness for the development of new imprinting strategies and for mechanistic studies (Bitas and Samanidou, 2018; Daniel et al.,

2005). When polymerization is carried out to use the materials in the monolithic form, (Özkara et al., 2011; Demiralay et al., 2010), bulk materials usually need to be crushed, ground and sieved to obtain particles of the desired size. Typically, this technique can only recover less than 50% of the polymer. Scaling presents difficulties in these circumstances. Numerous chromatographic and separation applications cannot be used because of the uneven size and form of the particles. During milling, certain binding sites can be damaged, which would significantly reduce the loading capacity (Gao et al., 2020; Otero-Romani et al., 2008).

2.7.2. Emulsion Polymerization

Emulsion polymerization is a heterogeneous polymerization process. Because it consists of two immiscible phases; one of them is a continuous phase and the other is a dispersed phase. In emulsion polymerization, water is generally used as the emulsion medium (dispersed phase). The monomer is dispersed in this medium with the help of an emulsifying agent. A water-soluble substance is used as the initiator. It is an emulsifying surfactant and contains hydrophilic and hydrophobic groups in its molecular structure. Most of the emulsifier's molecules aggregate to form small colloidal particles called micelles. A small part is soluble in water in molecular form. There is a dynamic balance between the emulsifier molecules in the solution and the micelles. If the amount of emulsifier is increased relative to the monomer, smaller-sized but much larger micelle particles are formed.

2.7.3. Suspension Polymerization

Like emulsion polymerization, suspension polymerization is a heterogeneous polymerization method. It also requires two immiscible phases. In suspension polymerization, the monomer is suspended in a suitable dispersion medium. Acrylic, methacrylic acids, styrene and its copolymers and many other unsaturated monomers are polymerized in this process. Initiators dissolved in monomer (benzoyl peroxide, Azobisisobuturonitrile (AIBN)) are used as initiators in polymerization. In order to stabilize the suspension and prevent the resulting polymer particles from sticking to each other, water-soluble stabilizers (such as carboxymethyl/cellulose, powdered potassium carbonate, and polyvinyl alcohol) are added to the medium. In this method, the heat of polymerization is removed by the water in the environment and precise temperature control is ensured. After its synthesis, no additional process is needed. Suspension polymerization is superior to other polymerization methods in this respect and is widely used in industry.

2.7.4. Precipitation Polymerization

Precipitation polymerization is defined as a homogeneous polymerization. The reason for this is that the medium initially consists of a homogeneous phase. The porogen dissolves all of the components (monomers, template molecule, and initiator), and polymerization begins as a homogenous solution. Precipitation polymerization is quite similar to bulk polymerization in practice, with the main variation being the quantity of porogen employed in the polymerization. A limited amount of solvent is used in bulk polymerization, but a substantial amount of porogen is used in precipitation polymerization.

The advantages of the technique can be listed as follows:

- The polymers generated are in particulate form,
- Almost all prepared materials are in a usable form,
- The template molecule can be more easily removed from the polymeric structure as they are not formed around a highly crosslinked polymer network,
- This method produces particles in the nano, submicron and micron range (Bitas and Samanidou, 2018).

The size and shape of the prepared particles are directly related to the ratio of monomers to solvent and the mixing rate of the polymerization mixture. It is quite normal to obtain submicron size particles in the form of agglomerates (Fasihi et al., 2011; Behbahani et al., 2012; Bitas and Samanidou, 2018).

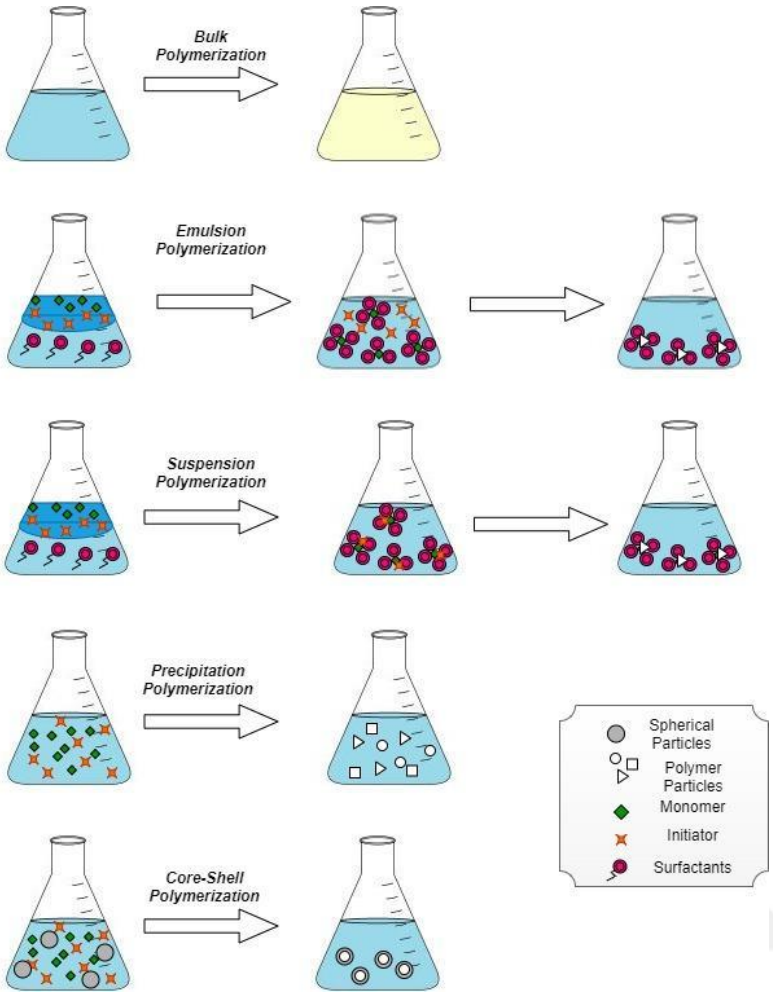

Figure 2.9. Polymerization Techniques of MIPs

3. MATERIALS AND METHOD

3.1. Materials

Chemicals used during the experiments; Angiotensin II (Ang II), Angiotensin I (Ang II) and Vasopressin (Vsp), and 1-Vinylimidazole (VIM) were provided from Sigma - Aldrich (St. Louis, MO, USA). Ethylene Glycol Dimethacrylate (EGDMA), poly(vinyl alcohol) (PVA), sodium dodecyl sulfate (SDS), 2-hydroxyethyl methacrylate (HEMA), Sodium bicarbonate, Sodium chloride, ammonium persulfate, Phosphate Buffer Saline (PBS) and ethanol were obtained from Sigma Chemical Co. (St. Louis, USA). Required solutions were prepared using ultrapure Type 1 water (UPW) with a conductivity of 18 MΩ-cm at room temperature and analytical grade reagents. All reagents were stored according to provided information and waste materials were disposed abiding by waste disposal regulations.

All chemicals used are of reagent-grade purity.

Devices used during the experiments; Glass polymerization reactor (Radleys Carousel 6 Plus Reaction Station), Homogenizer (BIOBASE D-160, Shandong, China), Centrifuge (Allegra X-30R, Beckman Coulter, USA), Shimadzu Type ATX224 No. D307039788 Electronic Balance, Scientific Vortex Mixer (Daihan, Korea), The GENESYS 150 UV-Vis Spectrophotometer (Thermo Fisher Scientific, USA), Oven (MIPROLAB MLF 120, TURKEY), Model of Millipore DIRECT-Q®3 ultrapure (type 1) water with BioPak®ultrafiltration cartridge with Millipak®Express 20 (0.22 µm) membrane filter, Scanning Electron Microscope (SEM) (FEI, Quanta 650 Field Emission SEM, USA), Zetasizer (Nano S-90, Malvern Instruments, London, UK), FTIR (Fourier Transform Infrared) spectrometer (Jasco FT/IR-6700, Japan), Hitachi HT-7700, Japan.

Basic laboratory equipment and consumables are not included.

3.2. Methods

3.2.1. Synthesis of Angiotensin II imprinted and non-imprinted pHEMA based nanoparticles (Ang II-MIPs$_{np}$-NIPs$_{np}$)

Ang II imprinted (Ang II-MIPs$_{np}$) and non-imprinted (NIPs$_{np}$) nanoparticles will be prepared to synthesize NPs that can specifically recognize to Ang II. Polymerization was carried out in the Radleys Carousel 6 Plus Reaction Station polymerization reactor (Figure 3.1), using the binary liquid phase mixture method (Baydemir et al., 2013). The first liquid phase is an aqueous solution (5 mL) of Polyvinyl alcohol (PVA) (100 mg), Sodium dodecyl sulfate (SDS) (15 mg) and sodium bicarbonate (12.5 mg). The second liquid phase is an aqueous solution (100 mL) of PVA (50 mg) and SDS (50 mg). The monomer phase is; Prepared using 1-vinyl imidazole (0.1 mL), 2-hydroxyethyl methacrylate (HEMA) (0.25 mL), Ethylene glycol dimethacrylate (EGDMA) (1 mL).

The prepared monomer phase was added to the first liquid phase. The mixture was homogenized at 30000 rpm for 30 min in a homogenizer (BIOBASE D-160, Shandong, China) to obtain a miniemulsion. Then, the mixing process was continued at 300 rpm in the first magnetic stirrer.

Figure 3.1. Radleys Carousel 6 Plus Reaction Station polymerization reactor

Meanwhile, Ang II:VIM (mole:mole) mixtures at 1:5, 1:10 and 1:20 mole ratios are prepared in order to determine the molar ratio in which Ang II and VIM molecules form the most effective pre-complex, and to stabilize the interaction. It was kept in the refrigerator at +4°C for 2 hours. In order to determine the most effective pre-complexing ratio, the pre-complex prepared at different ratios was compared in the UV spectrophotometer and the complexation ratio to be used in the study was decided (Fan et al., 2020; Çimen et al., 2020; Şener et al., 2010; Dai et al., 2018). The optimum molar ratio was determined as 1:10 (Ang II:VIM, mol:mol).

While the mixing process was continuing, firstly, the pre-complex containing the template molecule at a 1:5 mole ratio was added to the first liquid phase and mixed for 10 minutes in a magnetic stirrer. Thus, the first liquid phase containing the pre-complex was miniemulsified and then slowly added to the second liquid phase. Then, the total mixture obtained was transferred to the glass polymerization reactor and the reactor was heated at 40°C with mechanical stirring (400 rpm). Finally, sodium bisulfite (50 mg) and ammonium persulfate (75 mg) were added to the mixture to initiate the reaction. Polymerization was continued at 40°C for 24 hours.

Using the same method; The pre-complex containing the template molecule in a 1:10 mole ratio was added to the first liquid phase and mixed for 10 minutes on a magnetic stirrer. Thus, the first liquid phase containing the pre-complex was miniemulsified and then slowly added to the second liquid phase. Then, the total mixture obtained was transferred to the glass

polymerization reactor and the reactor was heated at 40°C with mechanical stirring (400 rpm). Finally, sodium bisulfite (50 mg) and ammonium persulfate (75 mg) were added to the mixture to initiate the reaction. Polymerization was continued at 40°C for 24 hours.

Again, with the same method, the pre-complex containing the template molecule at a 1:20 mole ratio was added to the first liquid phase and mixed in a magnetic stirrer for 10 minutes. Thus, the first liquid phase containing the pre-complex was miniemulsified and then slowly added to the second liquid phase. Then, the total mixture obtained was transferred to the glass polymerization reactor and the reactor was heated at 40°C with mechanical stirring (400 rpm). Finally, sodium bisulfite (50 mg) and ammonium persulfate (75 mg) were added to the mixture to initiate the reaction. Polymerization was continued at 40°C for 24 hours.

The same steps were followed for the synthesis of NIP_{np}, which did not undergo molecular imprinted and will be used as a control group, without adding AngII to the medium. The miniemulsified first liquid phase was slowly added to the second liquid phase. Then, the total mixture obtained was transferred to the glass polymerization reactor and the reactor was heated at 40°C with mechanical stirring (400 rpm). Finally, sodium bisulfite (50 mg) and ammonium persulfate (75 mg) were added to the mixture. Polymerization was continued at 40°C for 24 hours. synthesized.

Thus, a total of 4 different NPs were obtained.

Table 3.1. Nanoparticle nomenclature and content table

Nanoparticles	**Pre-complex ratio (n:n, mmol:mmol)**	**HEMA**	**EGDMA**	**VIM**	**Ang II**
Ang II-MIP-1_{np}	1:5	0.25 mL	1 mL	11 mmol	2.2 mmol
Ang II-MIP-2_{np}	1:10	0.25 mL	1 mL	11 mmol	1.1 mmol
Ang II-MIP-3_{np}	1:20	0.25 mL	1 mL	11 mmol	0.55 mmol
NIP_{np}	-	0.25 mL	1 mL	-	-

The synthesized NPs were washed 3 times with Ultrapure Water (UPW), 3 times with pure ethyl alcohol and again with UPW (20 mL each), to remove unreacted monomers, surfactants and impurities. For each washing step, the solution was centrifuged at 30000 rpm for 40 minutes and at the end of the time, the washing solution on the nanoparticles was carefully removed using a micropipette. After each cycle, new wash solutions were added to the NPs. In each step, the washing solution was measured in the spectrophotometer and these processes were continued until the absorbance value was zero.

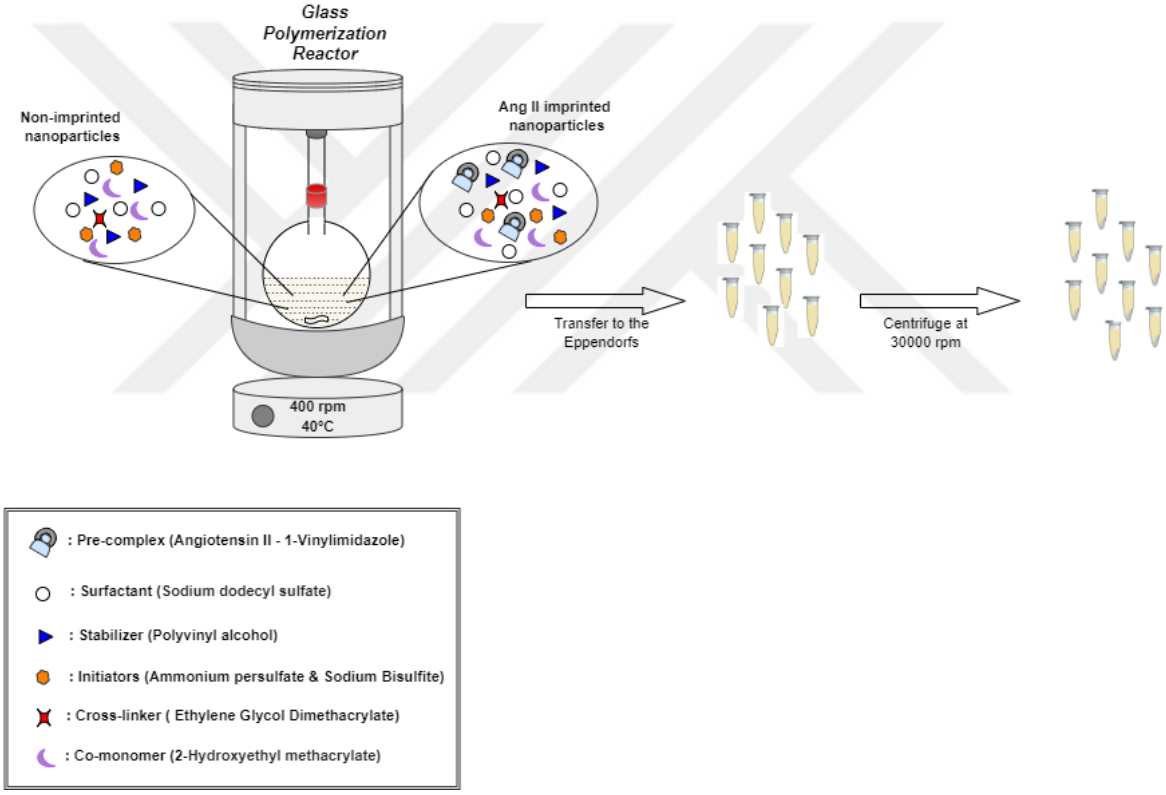

Figure 3.2. The polymerization process of Ang II-MIPs$_{np}$ and NIPs$_{np}$

3.2.2. Template Removal Studies

After the washing process is completed, in order to obtain Ang II specific cavities by removing the Ang II template molecule from the synthesized Ang II-MIPs$_{np}$ from the polymeric structure; NPs were reacted with PBS (10 mM, pH 7.4) elution solution containing 0.5 M NaCl. At this stage, 50 ml of elution solution was added to the NPs and dispersed in the elution solution in

an ultrasonic water bath for 15 minutes and then interacted with NPs in the rotator for 2 hours. It was then centrifuged at 30000 rpm for 40 minutes. The supernatant was measured spectrophotometrically at 195 nm, and the Ang II template molecule was removed until Ang II was not detected (Yıldırım and Pesint, 2020).

The removed Ang II amount Q_{tr} and the Ang II removal ratio (%) were calculated using following equations;

$$Q_{tr} = C_{Ang\ II} \times (V/m_{dry}) \quad (1)$$

$$\text{Removal ratio of Ang II (\%)} = (Q_r/Q_i) \times 100 \quad (2)$$

In Equation (1); $C_{Ang\ II}$ is Ang II concentration in elution medium in mg/mL, V is the volume of desorption agent in mL and m is the dry weight of the Ang II-$MIPs_{np}$ in g.

In Equation (2); Q_{tr} is Ang II removal amount (mg/g) and Q_i is the amount of Ang II in polymerization feed (mg/g).

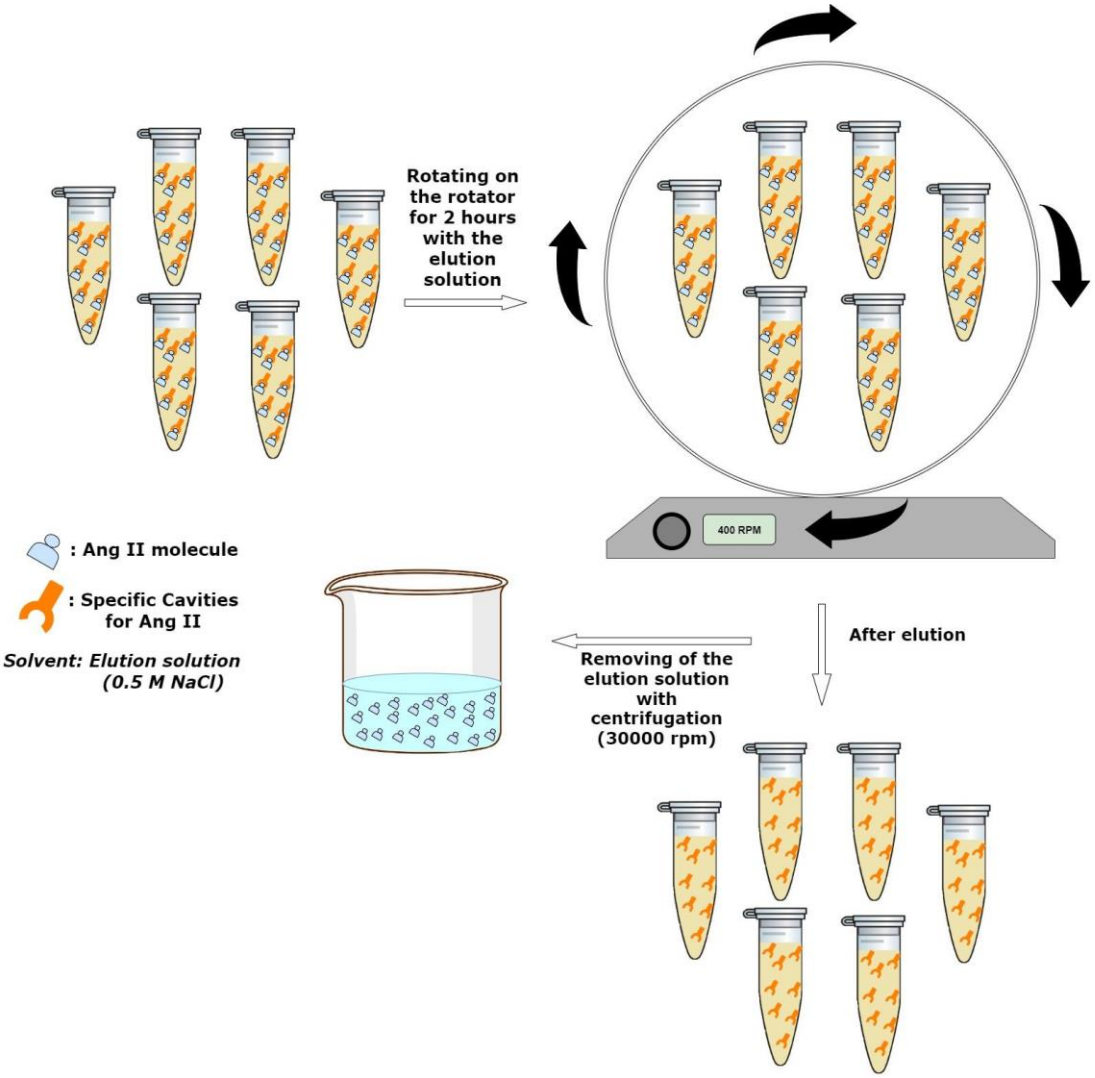

Figure 3.3. Template Removal. Schematic representation of template removal followed by formation of template-specific cavities

3.2.3. Characterization Studies

The polymerization yield of the NPs were calculated using polymerization feed amounts and dry particle weight and the surface area of the NPs was calculated using the density of the polymer and dimensional analysis results.

Zeta Dimension Analysis, Scanning Electron Microscopy (SEM), Transmission Electron Microscope (TEM), and FTIR spectrophotometer were used for the characterization of the prepared NPs. The sizes and size distribution of NPs prepared by particle size analysis were measured. Chemical structures of Ang II, VIM, Ang II:VIM complex, Ang II-MIPs$_{np}$ and NIPs$_{np}$ were analyzed comparatively in FTIR spectrophotometer. Large-scale images of NPs

were taken with SEM and TEM analyses and their particle sizes and morphological structures were shown (Baydemir et al. 2013, Ertürk et al., 2016, Battal et al., 2018).

3.2.3.1. Polymerization Efficiency

To calculate the polymerization efficiency of the synthesized NPs, first, the NP samples were swollen in 250 µL UPW and frozen at -16 °C, then lyophilized at 0.001 mbar and -50 °C for 24 hours to measure the dry weight of the NP samples.

$$\text{Polymerization Yield (\%)} = (m_{dry} / m_t) \times 100 \quad (3)$$

Here is m_t stands for the total mass of the monomers in the feed polymer mixture.

The surface area of NPs was calculated using the following expression (Bangs 1987; Çorman and Akgöl, 2012)

$$N = 6 \times 10^{10} S / \pi \rho_s d^3 \quad (4)$$

Here N is the number of nanoparticles per milliliter; S is the percentage of solids; ρ_s, the density of bulk polymer (g/mL); and d is the NPs diameter (µm). By multiplying N and the surface area of one NP, the specific surface area of Ang II-MIPs$_{np}$ was computed.

3.2.3.2. Particle Size Analysis

Dimensional analysis of synthesized Ang II-MIP$_{np}$ and NIP$_{np}$ was performed using Zetasizer Nano S-90 (Malvern Instruments, London, UK) in our Nanotechnology Application and Research Laboratory infrastructure. Particle size analysis makes nanoparticle size measurement using light scattering technique, and the experimental procedure followed for particle size analysis was briefly carried out as follows: The NP solution was prepared with water and 1.5 mL of it was taken and placed in the device housing. Light scattering occurred at an incidence angle of 90° and at 25°C. For data analysis, the viscosity and refractive index of deionized water were entered as 0.8822 (cP) and 1.33, respectively, and the absorption of the polymer as 0.001. The light scattering signal was calculated as the number of NPs per second and the instrument confirmed that the NP concentration in the solution was sufficient for the measurement. Each result was averaged by replicating three times and reported with standard deviation by the instrument software.

3.2.3.3. Surface Morphology

With SEM analysis, large-scale images of NPs were taken and particle sizes and morphological structures were shown. The scanning electron microscope (SEM) is a versatile advanced device that is frequently used to observe the surface morphology and composition of materials (Akhtar

et al., 2018). Morphological structures and particle sizes of Ang II-MIP_{np} and NIP_{np} were investigated using Scanning Electron Microscopy (FEI, Quanta 650 Field Emission SEM, USA) by purchasing service from Çukurova University Central Research Laboratory (Figure 3.4). Before SEM analysis, Ang II-MIP_{np} and NIP_{np} samples were prepared by dispersing them in an ultrasonic water bath in ethyl alcohol and dropped on a glass coverslip. Samples taken on a coverslip were dried in an oven (MIPROLAB MLF 120, TURKEY) at 40°C for 2 hours. After drying, the NP samples were fixed by passing them through a glass coverslip onto the SEM sample plate using a conductive adhesive to obtain SEM images. This step was carried out to ensure that the NPs were fixed as a thin layer as possible on the SEM sample plate. By coating the sample surface with gold under vacuum, the surface was made conductive and SEM images of the samples were taken at different magnifications.

Figure 3.4. FEI, Quanta 650 Field Emission SEM, USA

Transmission Electron Microscopy (TEM) analysis; It was carried out with the service procurement method with the Hitachi HT-7700 device located at Atatürk University (DAYTAM) in the Eastern Anatolia High Technology Research and Application Center. For this purpose, ethanol was added to the NPs and dispersed in ethanol by using an ultrasonic water bath. Then, the prepared NP solution was dripped onto the formvar film-coated copper grid and dried at room temperature. The dried NPs were then imaged to determine the particle size and size distribution.

Figure 3.5. Hitachi HT-7700, TEM, Japan

3.2.3.4. Structural Analysis

In the FTIR-ATR spectrophotometer, the chemical structure was analyzed by comparing the presence of the VIM functional monomer to be analyzed with the NIP_{np}. With this analysis, NPs that did not remove the target molecule Ang II were also analyzed and it was shown that the Ang II-VIM complex entered the NP structure. For the structural characterization of Ang II-MIP_{np} and NIP_{np}, FTIR (Fourier Transform Infrared) spectrometer (Jasco FT/IR-6700, Japan) was used by purchasing service from Çukurova University Central Research Laboratory. FTIR; It is a fast, harmless, time-saving analysis method that can detect the functional groups of solid, liquid or gaseous samples and is sensitive to changes in molecular structure (Cocchi et al., 2004). For the analysis of Ang II, VIM, Ang II-VIM pre-complex (1:10), Ang II-MIP_{np} and NIP_{np} samples, spectra were taken in the wavenumber range of 400-4000 cm^{-1}. NPs were ground into solid powder for analysis, while other samples were dissolved in ultrapure water.

Figure 3.6. Jasco FT/IR-6700, Japan

3.2.4. Adsorption Studies

The specific adsorption properties of Ang II-MIP$_{np}$ and NIP$_{np}$ for Ang II were studied with the batch system with Ang II aqueous solution at 25 °C (at pH 7.4). The effects of equilibrium Ang II concentration (50-500 pg/mL), interaction time (0-120 min) and temperature (4-40 °C) on Ang II adsorption were investigated.

3.2.4.1. Effect of Equilibrium Ang II concentration on Adsorption

Ang II-MIP$_{np}$ and NIP$_{np}$ were divided into equal amounts of eppendorfs by weighing. To evaluate the effect of equilibrium Ang II concentration on adsorption capacity, Ang II solutions of various concentrations ranging from 50-700 pg/mL (V: 1.5 mL) were added onto the NPs in the eppendorfs and interacted with the NPs at 400 rpm at 25 °C for 2 hours. Then the NPs were centrifuged at 30000 rpm and supernatants were taken for spectrophotometric measurement. The amount of adsorbed Ang II was measured spectrophotometrically by taking absorbance values at 195 nm wavelength.

For the adsorption capacities were calculated using;

$$Q = (C_o - C_f) * (V/m) \quad (5)$$

Here, Q is the amount of adsorbed Ang II for the unit mass of NPs (pg/g), C_o is concentrations of Ang II solutions measured before interaction with NPs (pg/mL) and C_f are concentrations of Ang II solutions measured after interaction with NPs for 2h (pg/mL), V is volume of the Ang II solutions (Adsorption solution) (mL), m is the dried mass of the NPs (g).

Experimental adsorption data were used and adsorption isotherms were used to examine the chemical and mechanical interaction behaviors between Ang II molecule and NPs. Langmuir and Freundlich adsorption isotherm models were used as the isotherm model in the thesis study.

The suitability of the adsorption properties of Ang II and NPs to these isotherms was evaluated. The adsorption mechanism has been explained using adsorption kinetic models.

3.2.4.2. Effect of the Temperature on Adsorption

Temperature studies were carried out with the 50 pg/mL Ang II determined. Temperature (4°C-40°C, 2 h) on adsorption rate and capacity were investigated under the same conditions. The initial absorbance value of Ang II concentration (50 pg/mL) was measured at 195 nm wavelength.

3.2.4.3. Effect of Interaction Time on Adsorption

Evaluation of the effect of interaction time on Ang II adsorption was carried out with 50 pg/mL Ang II. NPs were weighed and divided equally into 7 separate eppendorfs. 1.5 mL of Ang II solution was added onto the NPs in eppendorfs and interacted with the NPs at 25 °C at 400 rpm. The initial absorbance value of Ang II concentration (50 pg/mL) was measured at 195 nm. After stopping the interaction at 0, 5, 15, 30, 60, 90 and 120 minutes each, respectively, the samples were centrifuged at 30000 rpm. The resulting supernatants were measured spectrophotometrically at 195 nm. The absorbance values taken at different times were compared.

3.2.5. Selectivity Studies

In order to determine the specific Ang II molecule selectivity of Ang II-MIP$_{np}$, Ang I and Vsp molecules, which coexist in blood serum and are similar to Ang II in molecular structure and size, were selected as competitor molecules (Figure 3.4).

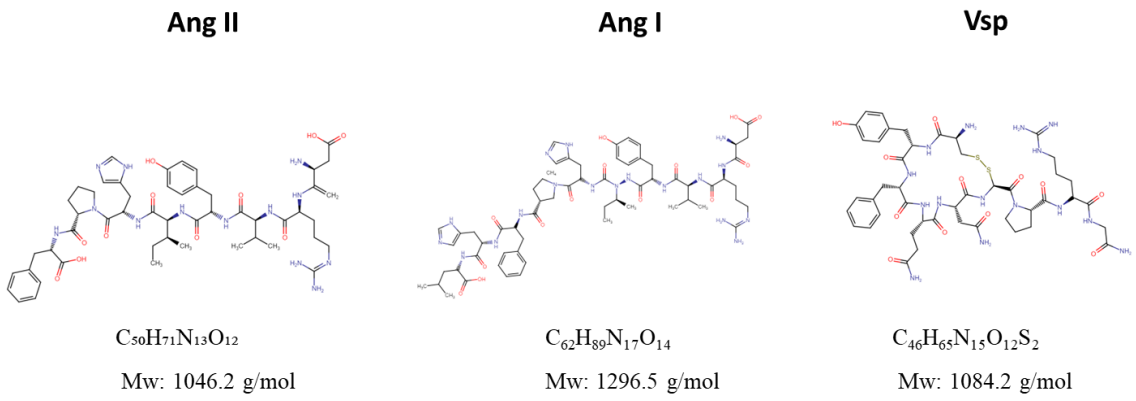

Figure 3.7. Molecular formulas of Ang I and Vsp

Three separate solutions of Ang II, Ang I and Vsp with the concentration of 40 pg/mL each 1.5 mL (pH 7.4), were prepared in order to evalute selectivity spectrophotometrically was prepared. 1.5 mL of each solution were added onto the NPs in the eppendorfs and interacted with the NPs at 400 rpm at 25 °C for 2 hours. Then the NPs were centrifuged at 30000 rpm and supernatants were taken for spectrophotometric measurement. The amount of adsorbed Ang II was measured spectrophotometrically by taking absorbance values at 195 nm wavelength and distribution coefficient (Q_d, mL/g) was calculated according to the following equation.

The distribution and selectivity coefficients of Ang I and Vsp with respect to Ang II were calculated as explained by the following equation;

$$Q_d = [(C_i - C_f) / C_f] \times V/m \quad (6)$$

Here, Q_d represents the distribution coefficient; C_i and C_f are the initial and final concentrations of biomolecules, respectively. V is the volume of the solution (mL) and m is the mass of nanoparticles used (g).

To evaluate the selective adsorption property of Ang II-MIP_{np}, the imprinting factor (IF) was calculated for Ang II and competitor molecules using the following equation;

$$IF = Q_{d\ (Ang\ II\text{-}MIPnp)} / Q_{d(NIP)} \quad (7)$$

$Q_{d\ (Ang\ II\text{-}MIPnp)}$ and $Q_{d(NIP)}$ represent the distribution coefficients of Ang II-MIP_{np} and NIP_{np}, respectively.

The selectivity coefficient for binding of Ang II in the presence of competitive biomolecules is obtained from the equilibrium binding data according to the following equation;

$$k = Q_d\,(template) / Q_d\,(competitor) \quad (8)$$

Where k is the selectivity coefficient and competitors; Ang I and Vsp biomolecules. A comparison of the k values of the $MIPs_{np}$ with those steroid molecules allows an estimation of the effect of imprinting on selectivity.

The relative selectivity coefficient k' (8) can be defined as:

$$k' = k_{imprinted} / k_{control} \quad (9)$$

3.2.6. Desorption and Reusability

The desorption studies of Ang II-MIP_{np} and NIP_{np} were also carried out with the batch system and using 0.5 M NaCl (pH: 7.4) desorption solution. 1.5 mL of desorption solution was added onto the NPs, rotated on the rotator at 400 rpm for 2 hours at 25 °C, activated to remove Ang II from the structure. The NPs were then centrifuged at 30000 rpm and supernatants were taken for spectrophotometric measurement. The amount of adsorbed Ang II was measured spectrophotometrically by taking absorbance values at 195 nm wavelength.

The desorption rate was calculated using the following equation.

$$Desorption\ Ratio\ (\%) = \frac{The\ amount\ of\ Ang\ II\ released\ into\ the\ medium\ by\ desorption\ (pg)}{The\ amount\ of\ Ang\ II\ retained\ by\ adsorption\ (pg)} \text{ x } 100 \quad (10)$$

3.2.7. Selective Ang II Rebinding From Human Serum

Selective Ang II binding from human serum was also performed in human serum diluted 1:20-fold with PBS buffer (10μmM, pH 7.4). The human serum sample was spiked with Ang II to 25 pg/mL and then diluted 1:20. 1.5 mL was taken from the prepared serum sample and was added to the Ang II-MIP_{np} (m_{dry}= 0.15 g). It was applied in a batch system for 2 hours. After 2 hours, the final serum sample was collected. All collected experimental samples were then analyzed by the sandwich ELISA method using the commercial Angiotensin II EIA Kit. All Ang II binding amounts were calculated by ELISA (Awareness Technology Inc.) according to the ELISA kit technical report (Montezano et al., 2014; Yıldırım and Pesint, 2020).

4. ANALYSIS AND DISCUSSION

Ang II is a RAAS active hormone and an important biomarker in the complex network of other endocrine, and paracrine systems, in which RAAS affects many tissue and organ systems. Ang II has been a key focus for clinical interventions targeting the RAAS and its pathogenic actions and plays an important role, particularly in cardiovascular, renal and hypertension research. The specific detection of Ang II in a short time has become very important nowadays. Within the scope of this thesis, for the rapid and reliable determination of the amount of Ang II molecules

in the blood; The synthesis, characterization, adsorption, selectivity and reusability studies of Ang II-MIPs$_{np}$ and NIPs$_{np}$ were carried out using molecular imprinting technique.

4.1. Synthesis of nanoparticles

Optical photographs of NPs obtained by preparing with four different polymerization recipes are given in Figure 4.1. It has been shown that nanoparticles are mechanically stable cross-linked structures after washing processes.

Figure 4.1. Optical photographs of nanoparticles (before centrifugation (A-C) - after centrifugation (B-D)); **(A-B):** Ang II-MIP-1_{np}, Ang II-MIP-2_{np}, Ang II-MIP-3_{np} ; **(C-D):** NIP_{np}

In order to determine the molar ratio in which Ang II and VIM molecules pre-complex most effectively, it is frequently used in the literature to determine the molar ratio in which the interaction between the functional monomer and the template molecule is most effective in the pre-complexing phase in molecular sequencing studies spectroscopic method was applied (Fan et al., 2020; Çimen et al., 2020; Şener et al., 2010; Dai et al., 2018). Ang II:VIM (n:n) mixtures at 1:5, 1:10 and 1:20 mole ratios were prepared and kept at +4°C for 2 hours. In order to determine the most effective pre-complexing ratio, different ratios of pre-complex prepared were compared in UV spectrophotometer. In this step, spectrum scanning of VIM and Ang II molecules was also performed and it was determined that the maximum absorption wavelength of Ang II molecule was 200 nm and the maximum absorption wavelength of VIM molecule was 232 nm. As a result of the measurement in the UV spectrophotometer, it was determined that the maximum absorption wavelength shifted to 228 nm with the pre-complexation between VIM and Ang II (Figure 4.2). This indicates an interaction between VIM and Ang II molecules. When the UV spectra of Ang II:VIM (n:n) mixtures in the ratios of 1:1, 1:5, 1:10 and 1:20 in the prepared pre-complexes are compared; It was concluded that the absorbance intensity increased with increasing VIM ratios in the pre-complex, but there was not much change between 1:10 and 1:20 mole ratios. It was determined that the most effective interaction between Ang II and VIM in pre-complexation was at 1:10 mole ratio, with low-intensity absorbance values observed at 1:1, 1:5 mole ratios and UV spectra fixed at 1:10 (Figure 4.2).

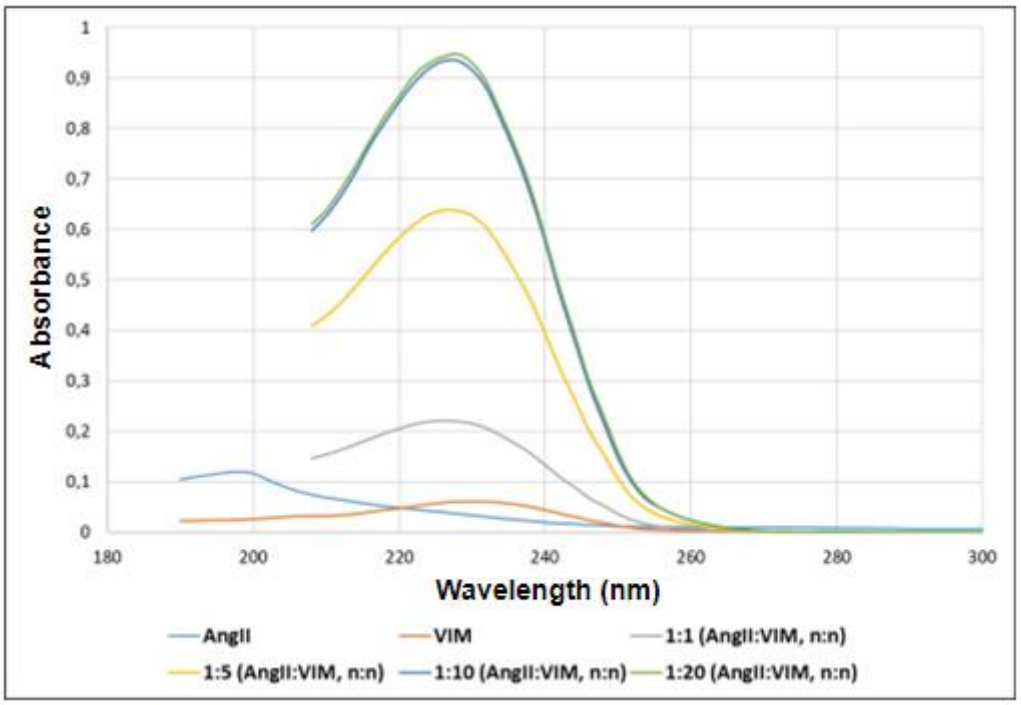

Figure 4.2. UV-VIS absorption spectra of Ang II:VIM (n:n) mixtures prepared in Ang II, VIM, 1:5, 1:10 and 1:20 ratios

4.2. Template Removal

The template remove of the Ang II molecule from the NPs was carried out with PBS (10 mM, pH 7.4) elution solution containing 0.5 M NaCl. The supernatant obtained in each step of the elution and washing processes was measured spectrophotometrically at 195 nm, and the removal of the template molecule was continued until Ang II was not detected (Yıldırım et al., 2020). The amount of Ang II removed from the NPs was determined spectroscopically and the results are summarized in Table 4.1.

Table 4.1. Ang II removal from nanoparticles

Nanoparticles	**Ang II:VIM ratio (n:n)**	**The amount of Ang II added in the polymerization step (mmol)**	**Amount of Ang II removed (mmol)**	**Ang II ratio removed (%)**
Ang II-MIP-1_{np}	1:5	2.2	1.6	72

Ang II-MIP-2_{np}	1:10	1.1	1.02	98
Ang II-MIP-3_{np}	1:20	0.55	0.47	85

According to the results obtained, the most effective template Ang II molecule removal from NPs was achieved at a ratio of 1:10 mole (98%). An effective Ang II-VIM interaction was not observed at 1:5 mole ratio as shown in Figure 4.2 and the low efficiency of removal of template molecule (72%) can be explained on this basis. It can be interpreted that the Ang II molecule could not be added to the structure as much as it was put into the polymerization medium, as a result of the pre-complex could not enter the NP structure while preserving its structure, and therefore the amount of Ang II removed from the structure was low. In 1:20 mole ratio, it can be said that the VIM molecule interacts with Ang II at a 1 mole ratio of 20 moles and the structure is quite stable with the secondary interactions between the molecules, and thus the pre-complex also participates in the polymer structure at this stability, but in this case, it is surrounded by VIM in the NP structure and is stable. It was observed that the Ang II molecules, which were kept in such a state, could not be removed from the structure with high efficiency with the elution solution (Table 4.1). For this reason, the efficiency obtained in the template molecule removal step performed until the absorbance is zero was found to be relatively lower (85%) for Ang II-MIP-3_{np} than for Ang II-MIP-2_{np}. At 1:10 mole ratio, the most effective complexation was observed (Figure 4.2), it can be interpreted that the pre-complex prepared at these ratios maintains its stability during the polymerization stage and the pre-complex placed in the polymerization medium is largely incorporated into the NP structure and the removal of the template molecule is more effective with the selected elution solution. The removal of the Ang II template molecule from the NP structure with 93% efficiency shows that Ang II-MIP-2_{np} is the polymer in which Ang II is removed from the structure in a good way and the cavities specific to this molecule are formed most effectively.

According to the results obtained, the Ang II-MIP-2_{np} was chosen to be used in the studies and continued to work with these NPs in the continuation of the experimental studies carried out within the scope of the thesis. In the continuation of the thesis, the selected NP is referred to as Ang II-MIP_{np}.

4.3. Characterization Studies

The graphs of the dimensional analysis results obtained from the Zetasizer device are given below. The size distributions of Ang II-MIP$_{np}$ and NIP$_{np}$ prepared under optimized polymerization conditions, respectively; It was found as 50.25 nm ve 51.97 nm (Figure 4.3).

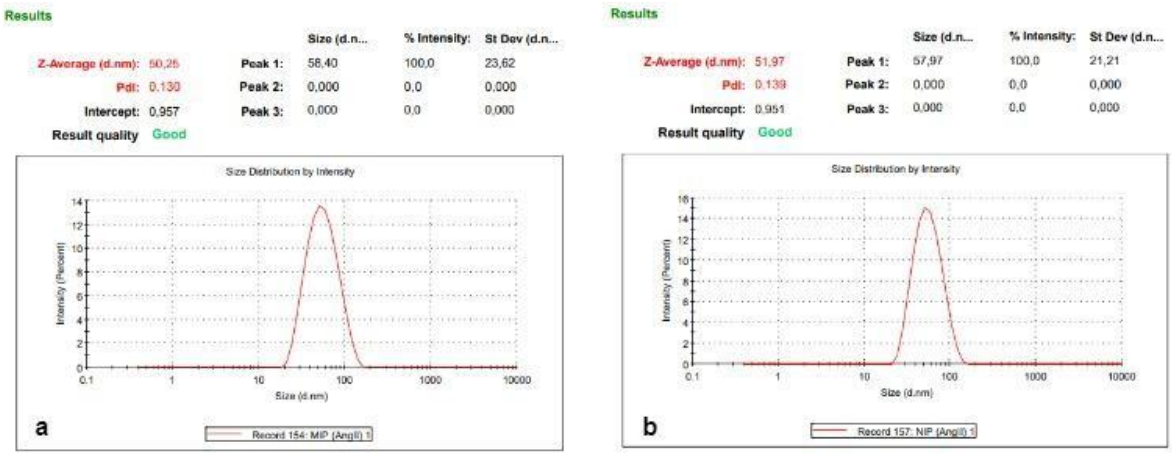

Figure 4.3. Particle size analysis of nanoparticles homogenized at 30000 rpm. (a) Ang II-MIP$_{np}$ (b) NIP$_{np}$

Ang II-MIPs$_{np}$ and NIPs$_{np}$ synthesized by emulsion polymerization are approximately 50 nm and 52 nm in size, respectively. The surface area of the NPs was calculated as 26903.4 m^2/g and 25868.9 m^2/g, respectively, with the help of equation number 4. The value found shows that a very large surface area can be achieved when compared with the studies in the literature. The large surface area value ensures that very high adsorption capacities can be achieved as it keeps the mass transfer limitations to a minimum.

Table 4.2. Polymerization yield and surface area of Ang II-MIPs$_{np}$ and NIPs$_{np}$

Polymers	Polymerization Yield, %	Surface area (m^2/g)
NIP$_{np}$	98.36	25868.9
Ang II-MIP$_{np}$	96.87	26903.4

SEM images of the samples were taken at different magnifications and the surface was made conductive by coating the sample surfaces with gold under vacuum. When SEM images were examined, it was observed that Ang II-MIP_{np} and NIP_{np} sizes were around 50 nm and the size distribution was homogeneous. Ang II-MIP_{np} and NIP_{np} have similar structures and similar size distributions (Figure 4.4).

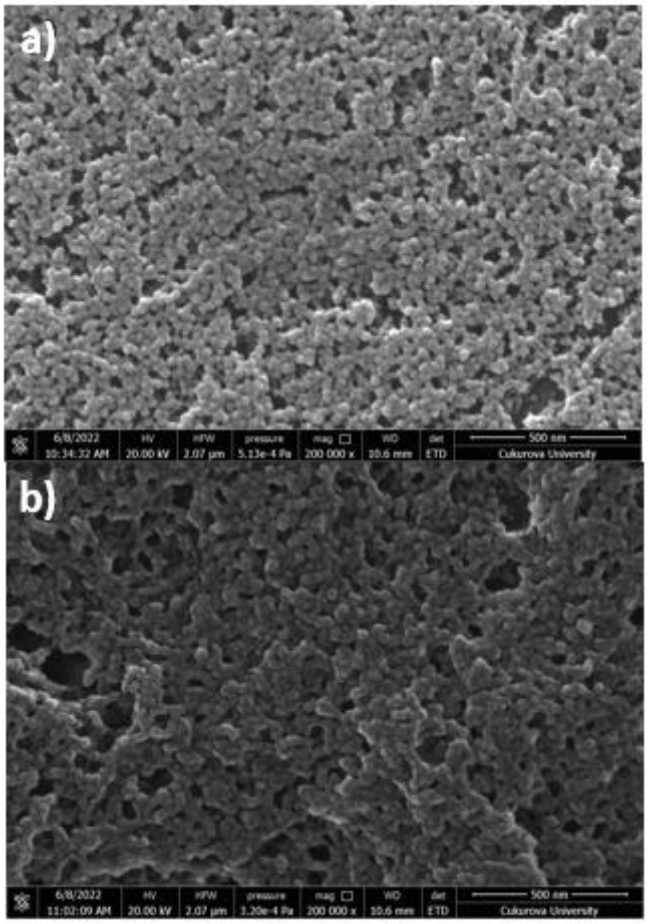

Figure 4.4. (a) Ang II-MIP_{np} SEM images 200,000X, (b) NIP_{np} SEM images 200,000X

TEM analysis shows that the NPs have a size of around 50 nm and a spherical shape (Figure 4.5). The mean particle size was determined after at least 30 measurements with the Image J program. Results from Zetasizer showed that Ang II-MIP_{np} and NIP_{np} have average particle sizes of 50.25 nm ve 51.97 nm, respectively. The TEM photograph of NPs also confirms this result obtained from the Zetasizer device. TEM photographs show that the synthesized NPs are in spherical form with a rough surface. TEM analysis also confirms the result that the applied polymerization protocol is suitable for synthesizing NPs with a size of around 50 nm.

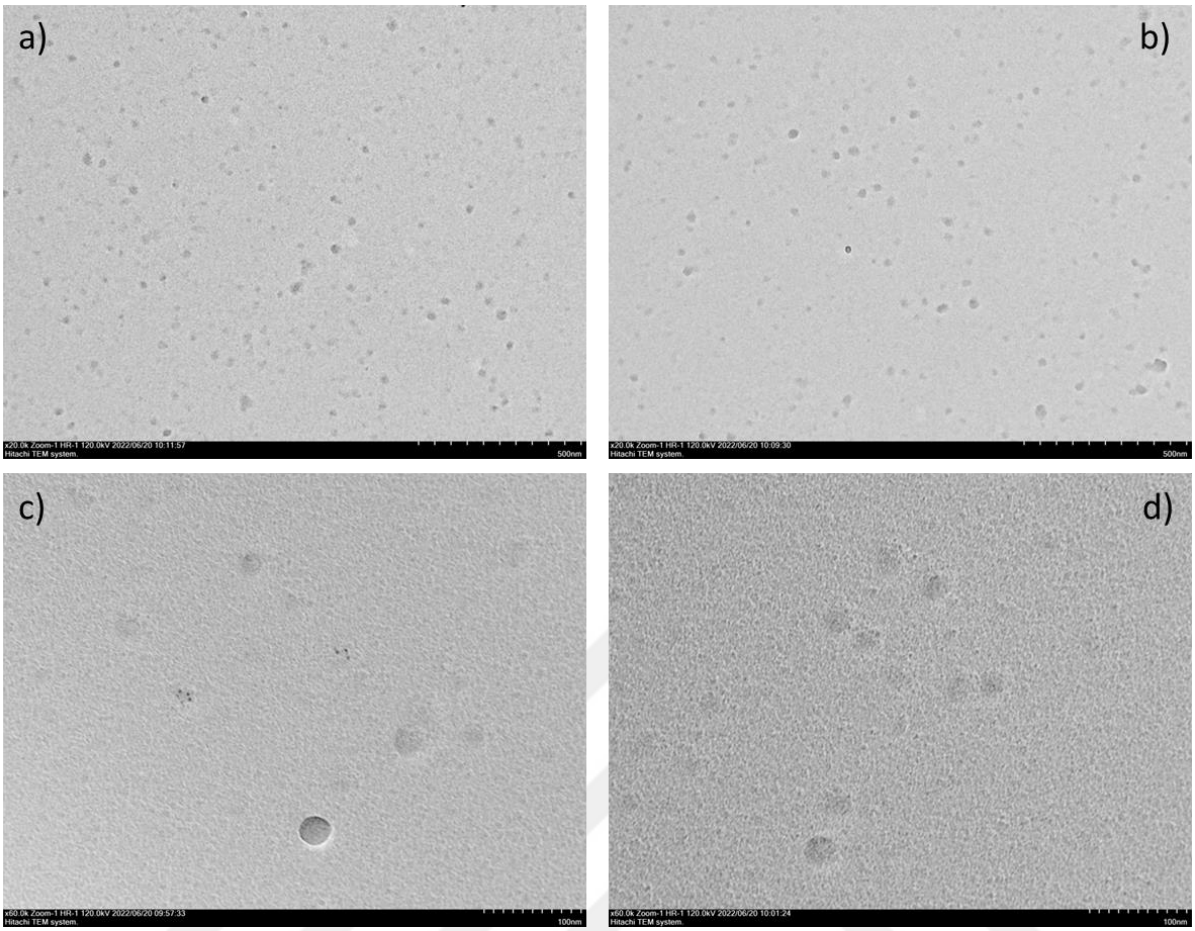

Figure 4.5. TEM photographs of Ang II-MIP$_{np}$ and NIP$_{np}$. **a,c)** Ang II-MIP$_{np}$ (x20 and x60 zoom); **b,d)** NIP$_{np}$ (x20 and x60 zoom)

In the FTIR-ATR spectrophotometer, the chemical structure was analyzed by comparing the presence of the VIM functional monomer to be analyzed with the NIP$_{np}$. With this analysis, NPs that did not remove the target molecule Ang II were also analyzed and it was shown that the Ang II-VIM complex entered the NP structure. Spectra of Ang II, VIM and Ang II-VIM pre-complex (1:10) are given below, respectively (Figure 4.6).

When the FTIR spectrum of Ang II is examined; There are bands of C=C stretching around 1600 cm^{-1} and aromatic C-H bending around 1500 cm^{-1}, and it is also seen that it gives a spectrum in the range of 3600-3500 cm^{-1} due to O-H stretching vibrations (Tekin et al., 2011). Ang II has a C-H stretch band at about 2960 cm^{-1}, a C=C stretch band around 1625 cm^{-1} and a N-H bending band. The stresses of the C=N-C aromatic ring are observed around 1512 cm^{-1} in Ang II and around 1504 cm^{-1} in VIM, respectively. C-H ring bending at about 1112 cm^{-1} and C-N- ring bending at about 1024 cm^{-1} are observed at different intensities in both Ang II and VIM. There are C-H stretching vibrations at 2950 cm^{-1} and C-O stretching around 1249 cm^{-1}

for both Ang II and VIM. In the spectrum of VIM, there is a clearly visible N-H stretch band in the range of 2820–3000 cm^{-1} and a carboxylic acid O-H stretch band at 3112 cm^{-1} (Daoud-Attieh et al., 2013). When the FTIR spectrum of Ang II-VIM pre-complex is examined; After the complexation, a very large peak is observed due to O-H stretching around 3400 cm^{-1}. It can be said that the reason for the increase in the intensity of this peak and its shift to higher frequencies is due to the H bond resulting from the complexation. In addition, after complexation, the C=N stretch band shifted to the left and the peak in the C=N-C- aromatic ring stretch band also increased in intensity and shifted to higher frequencies. Considering all these changes, it can be said that Ang II and VIM successfully formed a preliminary complex. The characteristic FTIR spectra of Ang II-MIP_{np} and NIP_{np} are given below (Figure 4.6 - 4.7). Because the structures of Ang II-MIP_{np} and NIP_{np} are quite similar, their spectra are very similar. Although the intense HEMA and EGDMA content in the structure screens the VIM and Ang II molecules that enter the structure, the presence of these molecules has been successfully demonstrated. O-H stretching bands seen around 3404 cm^{-1} belong to the hydroxyl group originating from HEMA common in their structure, aliphatic C-H stretching bands around 2950 cm^{-1} due to the methyl group in HEMA and EGDMA, the carbonyl group of EGDMA around 1720cm^{-1} C=O stretch bands of the double bond; C-O stretch bands around 1130 cm^{-1} from EGDMA are common bands seen in both spectra. Unlike NIP_{np}, the bands seen in Ang II-MIP_{np} at 1222 cm^{-1} and 1203 cm^{-1} are amine group stretching bands, indicating amine groups in imprinted cavities, and this may be evidence of Ang II-MIP_{np} making more H bonds than NIP_{np}. The band around 1635 cm^{-1} is due to vibrations of aromatic and aliphatic double bonds (C=C, C=N), which are thought to originate from Ang II-VIM pre-complex in Ang II-MIP_{np} structure. In addition to these, the peak intensity of the C-O group seen around 1250 cm^{-1} is higher in Ang II-MIP_{np} than NIP_{np} and it shifts to a higher frequency than NIP_{np}, and the peaks of the carboxyl group of VIM at 1130 cm cm^{-1} are higher. Its existence can also be explained by the inclusion of the VIM molecule in the structure. However, the shift of the frequency at 1710 cm^{-1}, which is caused by C=O vibrations, to a higher frequency in Ang II-MIP_{np} and the fact that the peak intensity is different from NIP_{np} supports the presence of the pre-complex molecule in the structure. These changes observed in the spectra indicate that Ang II-VIM pre-complex is incorporated into the structure of Ang II-MIP_{np}.

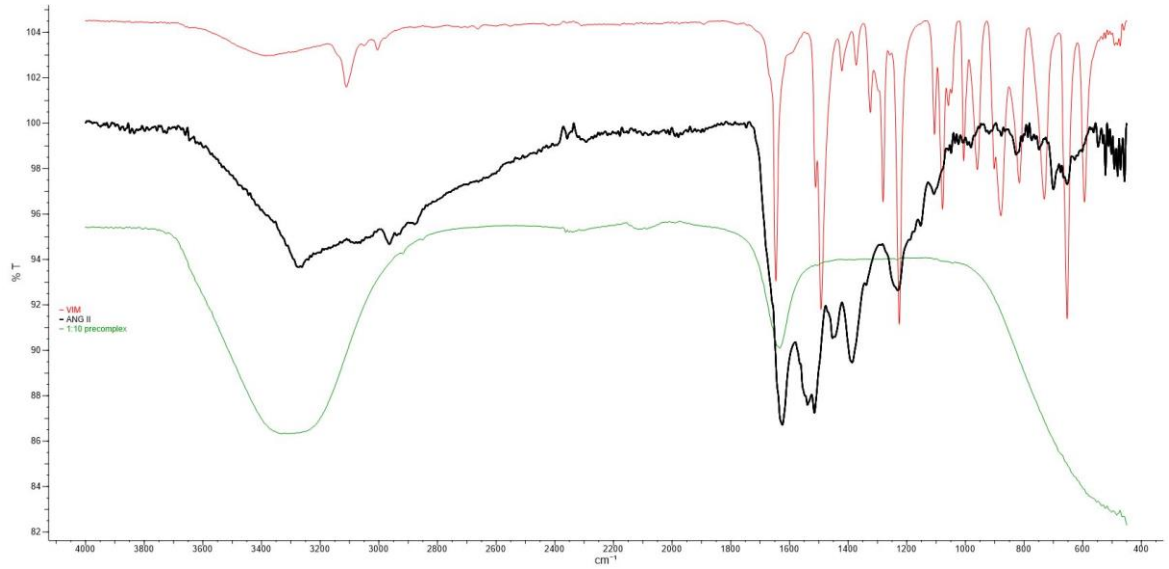

Figure 4.6. FTIR Spectrum of Ang II, VIM and 1:10 Ang II:VIM (n:n) pre-complex

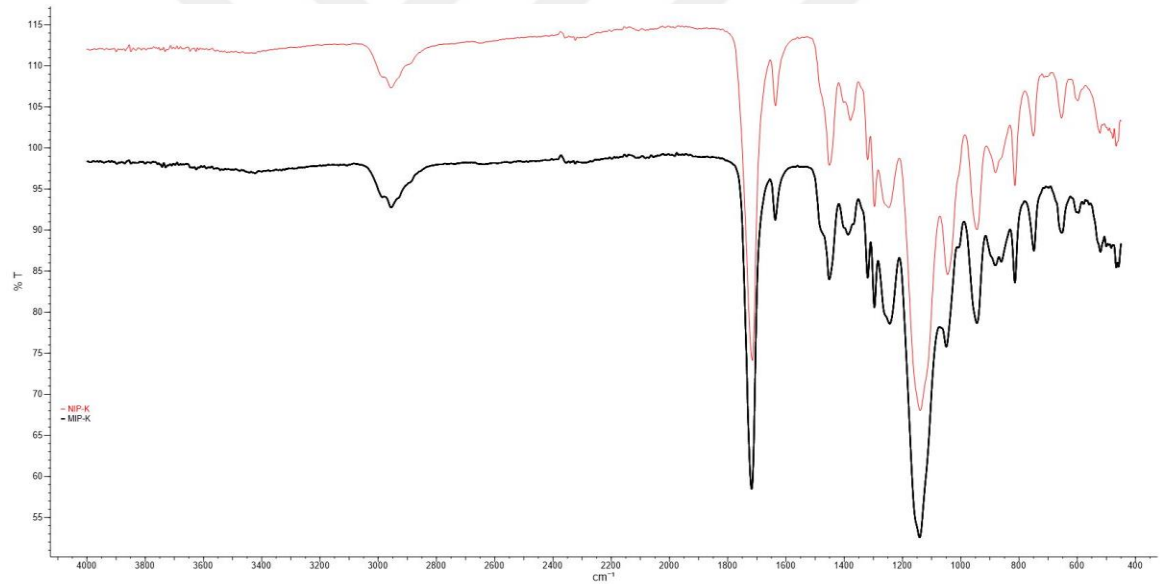

Figure 4.7. FTIR Spectra of Ang II-MIP_{np} and NIP_{np}

4.4. Adsorption Studies

4.4.1. Effect of Equilibrium Ang II Concentration on Ang II Adsorption

The initial Ang II concentration was changed in the range of 50-700 pg/mL and the Ang II adsorption capacity of the NPs was investigated. For Ang II-MIP_{np} and NIP_{np}, it appears that the adsorption of Ang II per gram polymer increases as the initial amount of Ang II increases (Figure 4.8).

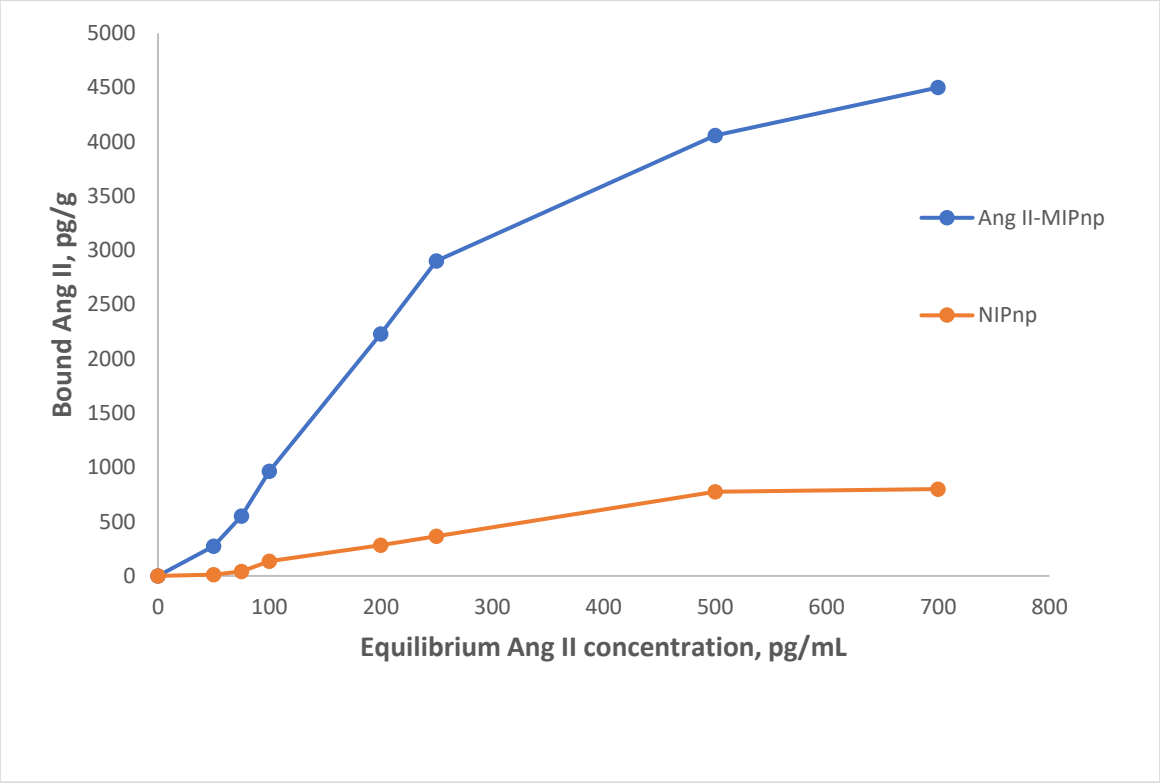

Figure 4.8. Effect of equilibrium Ang II concentration on Ang II adsorption of Ang II-MIP_{np} and NIP_{np}. mdry: 0.0754 g, V: 1.5 mL, time: 120 min, T: 25 °C, pH: 7.4, rotating: 400 rpm

4.4.2. Effect of Temperature on Ang II Adsorption

The effect of temperature on Ang II adsorption was investigated in the range of 4-40 °C. The effect of temperature on Ang II adsorption of Ang II-MIP_{np} is given in Figure 4.9. As seen in Figure 4.9, the increase in temperature increased the adsorption, but the increase in temperature after 25°C adversely affected the adsorption capacity. The maximum adsorption value observed at 25°C is 275.3 pg/mL. The lowest adsorption value was 118.1 pg/mL observed at 4°C.

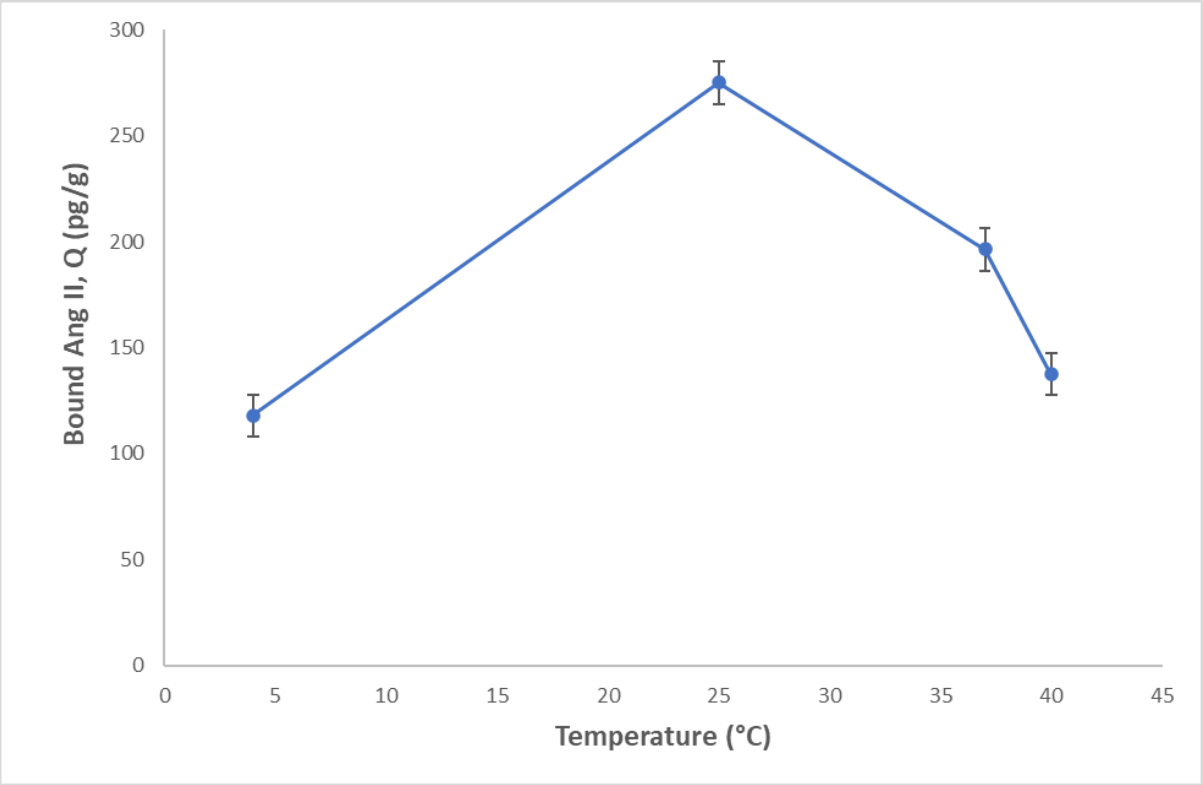

Figure 4.8. Effect of the temperature on Ang II adsorption of Ang II-MIP$_{np}$. Ang II Concentration: 50 pg/mL, mdry: 0.0754 g, V: 1.5 mL, time: 120 min, pH: 7.4, rotating: 400 rpm

4.4.3. Adsorption Isotherms

The interaction behavior between adsorption isotherms and NPs and Ang II molecules was investigated, using the experimental adsorption data obtained in section 4.4.1. Adsorption isotherms basically reveal the relationship between the amount of adsorbate (Qe) adsorbed on the adsorbent and the equilibrium concentration (Ce) of the adsorbate in the solution (Zenger and Peşint, 2022). In this study, the interaction was investigated using Langmuir and Freundlich adsorption isotherm models.

The Langmuir model is based on the homogeneity assumption, such as equally accessible adsorption sites, monolayer surface coverage, and no interaction between adsorbed species (Foo and Hameed, 2010; Mohann et al., 2006). The Langmuir model has been widely used for bonding isotherms using molecularly imprinted polymers (Li and Husson, 2006). This model is defined by the following equation.

$$Ce/Qe = 1/QL + 1/QL*b*Ce \quad (11)$$

Here; Qe is the concentration of Ang II bound to the adsorbent at equilibrium (pg/g); Ce, equilibrium Ang II concentration in solution (pg/mL); b is the Langmuir constant (mL/mg is a constant related to the free energy or net enthalpy of adsorption) and QL is the maximum Ang II adsorption capacity (pg/g). This equation can be linearized as follows:

When Ce versus Ce/Qe is plotted, the intersection of the line formed gives 1/QL*b, and its slope gives 1/QL.

Figure 4.9 shows the Langmuir adsorption isotherm of Ang II adsorption of Ang II-MIP_{np}. The maximum Ang II adsorption capacity (QL) was found to be 5.4 pg/g, and the Langmuir constant (b) was 620 mL/pg from the slope and cut of the graph.

In contrast to the Langmuir adsorption isotherm model, the Freundlich isotherm model is generally applied to heterogeneous adsorption systems. The amount of adsorbed substance is the sum of the adsorption at all sites. The Freundlich isotherm describes reversible adsorption and cannot be limited to the formation of a monolayer. According to this model, active binding sites that are close to each other interact with each other. The equation for the Freundlich adsorption isotherm is as follows:

$$\ln Qe = \ln Qf + 1/n^* \ln Ce \quad (12)$$

Here Qe is the amount of Ang II adsorbed per unit mass of adsorption at equilibrium (pg/g); Ce is the equilibrium concentration of Ang II in solution (pg/mL); Qf is the relative adsorption capacity constant of the adsorbent (pg/g); 1/n is the adsorption intensity constant. When plotting lnCe against lnQe, the slope of the line formed gives 1/n, and the intersection of the line gives lnQf.

Figure 4.10 shows the Freundlich adsorption isotherm of Ang II adsorption of Ang II-MIP_{np}. The 1/n was found 1.088 and the maximum Ang II adsorption capacity (Qf) was found to be 5,68 pg/g, from the slope and cut of the graph.

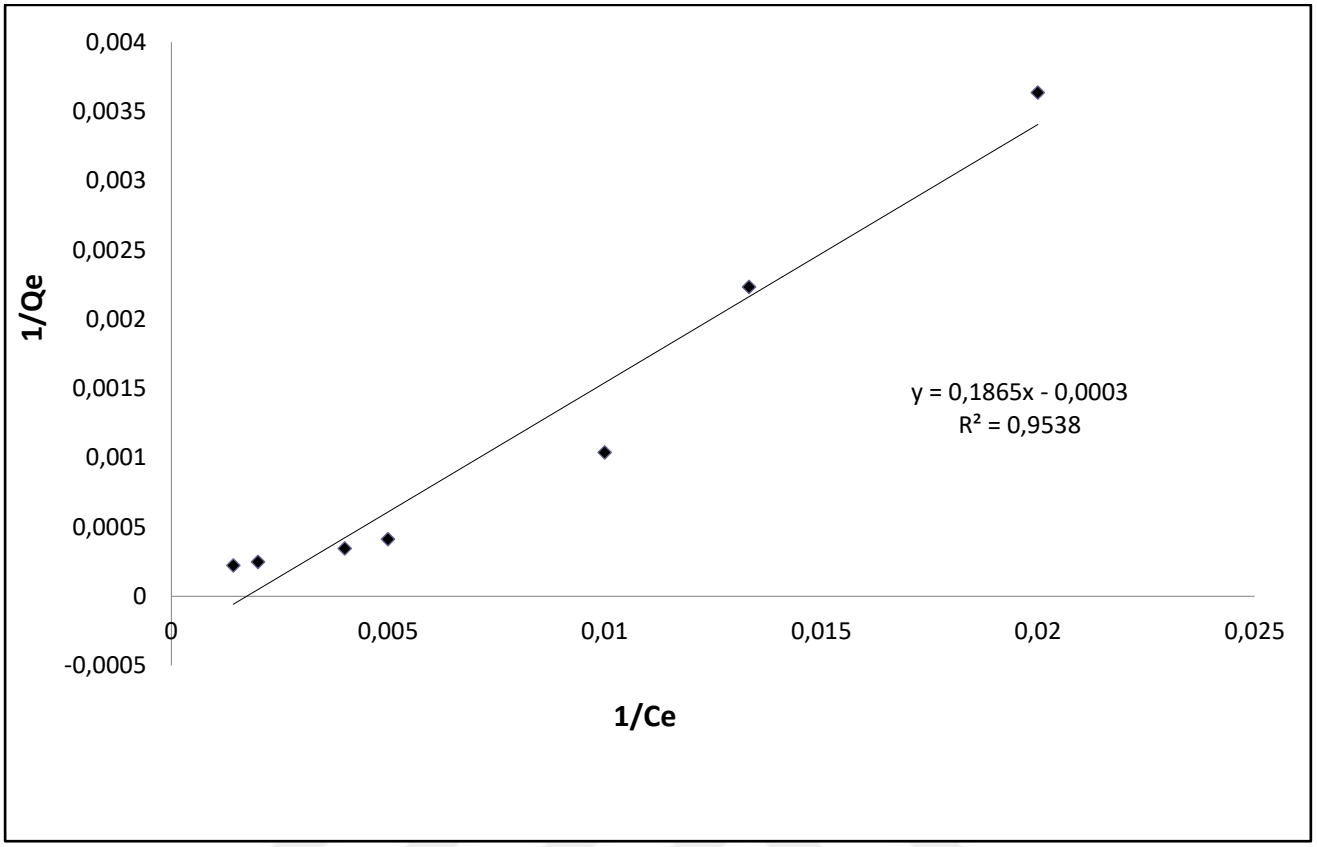

Figure 4.9. Langmuir adsorption isotherms of Ang II imprinted NPs

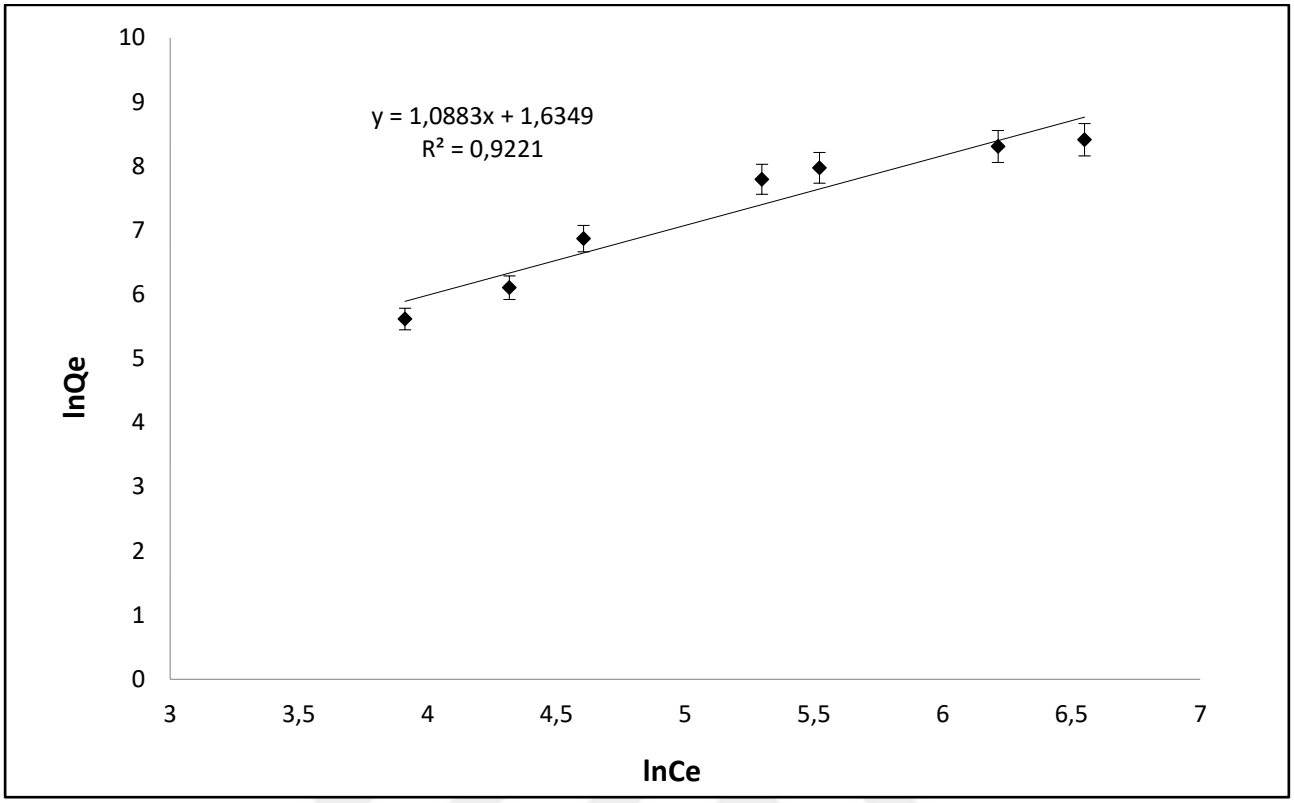

Figure 4.10. Freundlich adsorption isotherms of Ang II imprinted NPs

Ang II adsorption data were applied to Langmuir (Figure 4.9) and Freundlich (Figure 4.10) adsorption isotherms and by looking at the R2 values of the graphs obtained, it was found that Ang II adsorption conformed to the Langmuir isotherm. This result shows that Ang II binding sites on the surface of prepared Ang II imprinted NPs are homogeneously distributed, monolayer, equi-energy and with minimal lateral interaction. The results obtained from both isotherm models are given in Table 4.3.

Table 4.3. Langmuir and Freundlich adsorption parameters of Ang II-MIP_{np}

Experimental	Langmuir Constants			Freundlich Constants		
Qe	QL	b (mL/pg)	R2	Qf	n	R2
275	5,4	620,00	0,95	5,68	0,94	0,92

4.4.4. Effect of Interaction Time on Ang II Adsorption

The time dependence of Ang II adsorption on Ang II-MIP$_{np}$ was investigated and it was observed that the adsorption capacity increased with time and reached a maximum at the 120th minute (Figure 4.11). Pseudo-first and pseudo-second-order kinetic models were applied to the experimental data obtained. The rapidity of adsorption is related to the nanoparticle geometry and the imprinted regions on the surface and/or near the surface. The fact that the interaction sites are on the surface removes diffusion restrictions and allows rapid desorption kinetics.

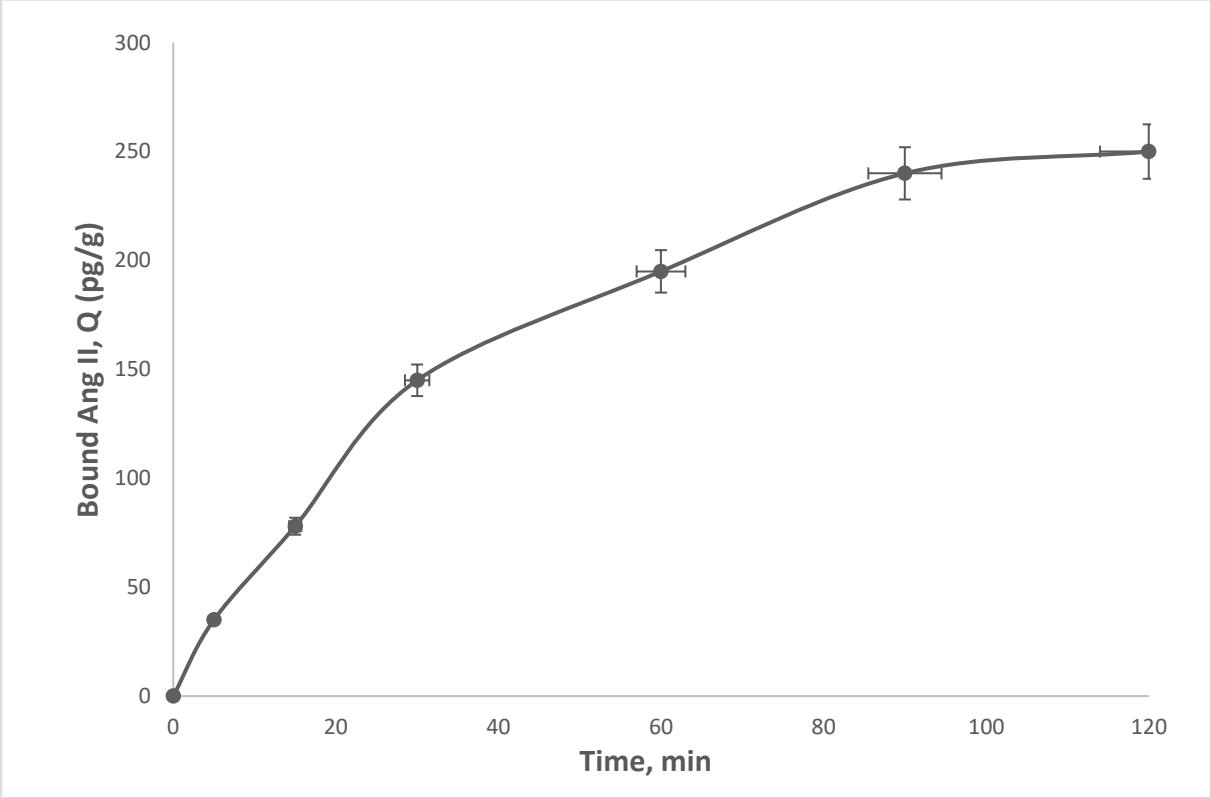

Figure 4.11. The effect of time on Ang II adsorption to Ang II-MIP$_{np}$. Initial Ang II concentration: 50 pg/mL; pH: 7.4 temperature: 25°C

Adsorption kinetics is a method in which the number of molecules attached to the solid-solution interface is used to reveal the mechanism of the reaction during adsorption. By using kinetic models, the mechanisms controlling the adsorption mechanism (mass transfer, diffusion-controlled chemical reaction) can be evaluated. In this direction; The experimental time-adsorption amount data were applied to the first- and second-order kinetic models to identify the mechanisms controlling the adsorption process.

In this study, Lagergren's first-order rate equation, whose equation is given below, is used.

$$\Delta Qt/dt = k1*(Qe-Qt) \quad (13)$$

In here, k1 is first order adsorption rate constant (min^{-1}); Qe and Qt are Ang II adsorption amount at equilibrium and at time t (pg/g), respectively. This equation was linearized as equation 14 and plotted log(Qe-Qt) versus t to obtain Qe and k1 from the cut-off point and slope.

$$\log(Qe-Qt) = \log(Qe) - (k1*t)/2.303 \quad (14)$$

The pseudo-second-order equation expressed as:

$$\Delta Qt /dt = k2*(Qe-Qt)^2 \quad (15)$$

k2 is pseudo-second-order adsorption rate constant (g mg^{-1} min^{-1}).

It was linearized as equation 16 and plotted (t/Qt) versus “t” to obtain “Qe” and “k2” from the cut-off point and slope;

$$(t/Qt) = (1/k2*Qe^2) + (1/Qe)* t \quad (16)$$

Pseudo first and pseudo-second-order kinetic plots are given in Figures 4.12. In Table 4.4, the rate constants obtained from these graphs and the adsorbed Ang II amounts at the experimental and equilibrium time are given. In the light of the data obtained, it is seen that the correlation coefficients found for pseudo-second-order kinetics are higher than those found for pseudo-first-order kinetics. In addition, the fact that the experimental Qe values are closer to the Qe values found for pseudo-second-order kinetics shows that adsorption is suitable for pseudo-second-order kinetics. This indicates that the rate-determining step during the adsorption process is the chemically controlled adsorption of Ang II imprinted particles.

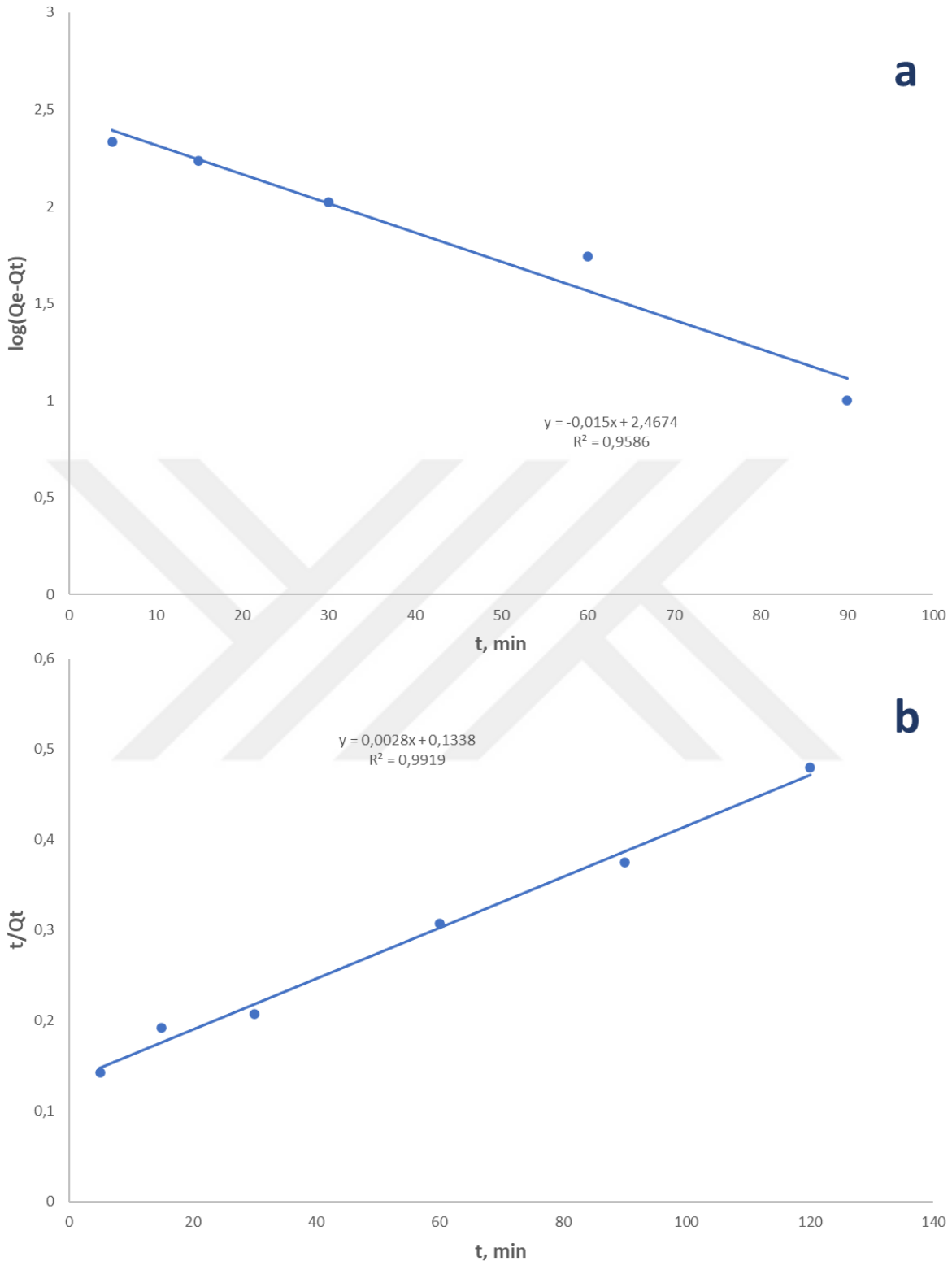

Figure 4.12. Adsorption Kinetics. The plot of a) pseudo-first-order kinetics and b) pseudo-second-order kinetics

Table 4.4. Adsorption Kinetics. Adsorption kinetics model constants and adsorption amount

Initial Conc. (pg/mL)	Exp.	Pseudo-first-order-kinetic			Pseudo-second-order-kinetic		
	Q_{eq} (pg/g)	k1 (1/dk)	Q_{eq} (pg/g)	R^2	k2 (1/dk)	Q_{eq} (pg/g)	R^2
50,00	250	0,035	11,8	0,96	0,000001	357,1	0,99

4.5. Selectivity Studies

In order to demonstrate the selectivity of synthesized Ang II-$MIPs_{np}$ and $NIPs_{np}$ against Ang II, competitive adsorption experiments were carried out in batch system with 40 pg/mL Ang II under equivalent conditions. Selectivity experiments were performed with aqueous solutions of Angiotensin I and Vasopressin separately. Ang I and Vsp have been chosen as competitors because they have similar molecular weight, similar size and shape to Angiotensin II.

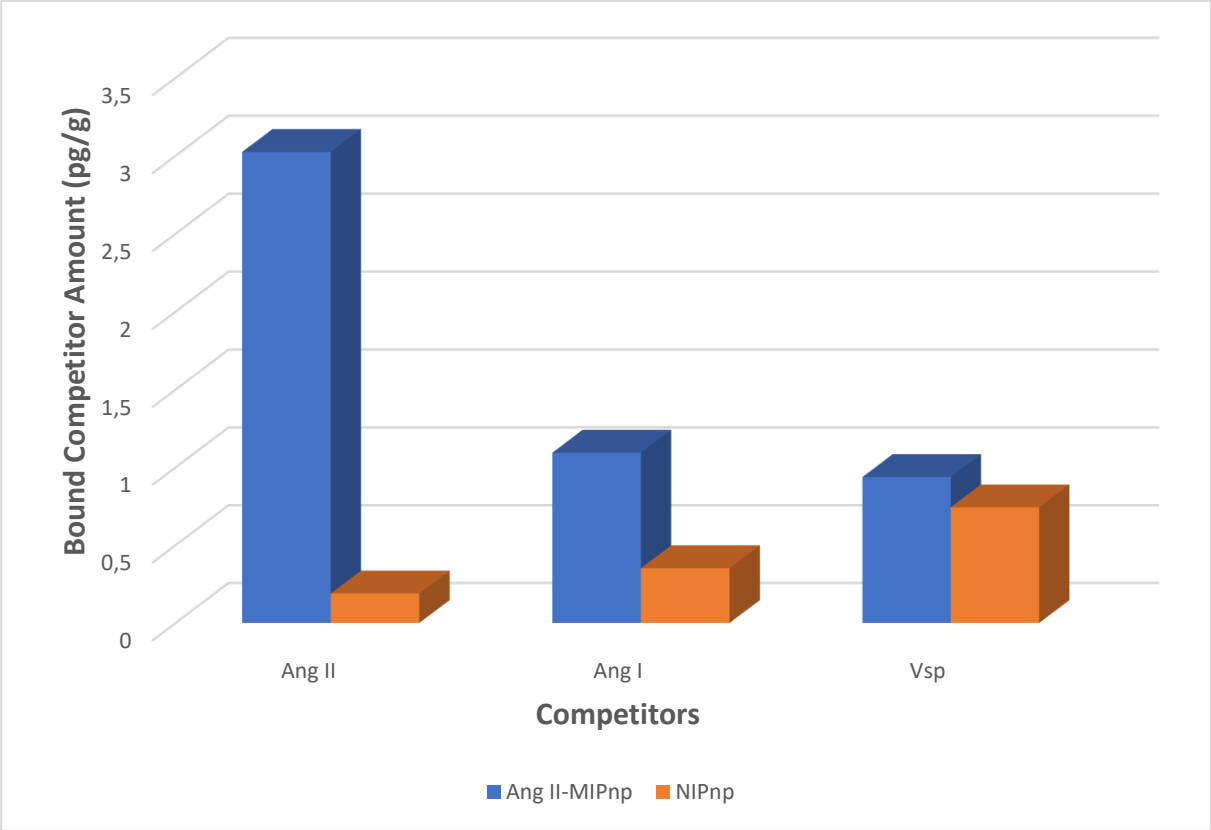

Figure 4.13. Selectivity Studies. Concentrations of each Ang II, Ang I and Vsp solution: 40 pg/mL, mdry: 0.0754 g, V: 1,5 mL, pH 7.4, time: 120 min, rotating: 400 rpm, T: 25°C

Calculations were made using equations 6,7,8 and 9. Selectivity coefficients calculated for Ang II-MIPs$_{np}$ are 2.76 for Ang I; 3.23 for Vsp. For NIPs$_{np}$, it was found to be 0.54 and 0.25, respectively. Relative selectivity coefficient showing imprinting selectivity was calculated as 5.14 (Ang II/ Ang I) and 12.66 (Ang II/ Vsp). Relative selectivity values; Ang II-MIPs$_{np}$ was 5.14 times more Ang II than Ang I; According to Vsp, it means that it recognizes with a selectivity of 12.66 times. The relative selectivity value is expected to be above 1, with the increase of the value, the efficiency of the imprinting process increases in direct proportion (Zhang et al., 2002).

Table 4.5. Selectivity. Selectivity and relative selectivity coefficients for Ang I and Vsp relative to Ang II

Molecule	Ang II-MIP$_{np}$		NIP$_{np}$		k'	IF
	Q_d (mL/pg)	k	Q_d (mL/pg)	k		
Ang II	3,02		0,19			15,98
Ang I	1,09	2,76	0,35	0,54	5,14	3,11
Vsp	0,94	3,23	0,74	0,25	12,66	1,26

4.6. Desorption and Reusability Studies

Reusability is very important for biomaterials. The adsorption and desorption processes of Ang II aqueous solution to NPs were repeated for 10 cycles using the same NPs in each cycle. The desorption rate was found to be 98%. As seen in the graph in Figure 4.14, The observed reduction in the amount of Ang II adsorbed over 10 cycles was quite small and acceptable.

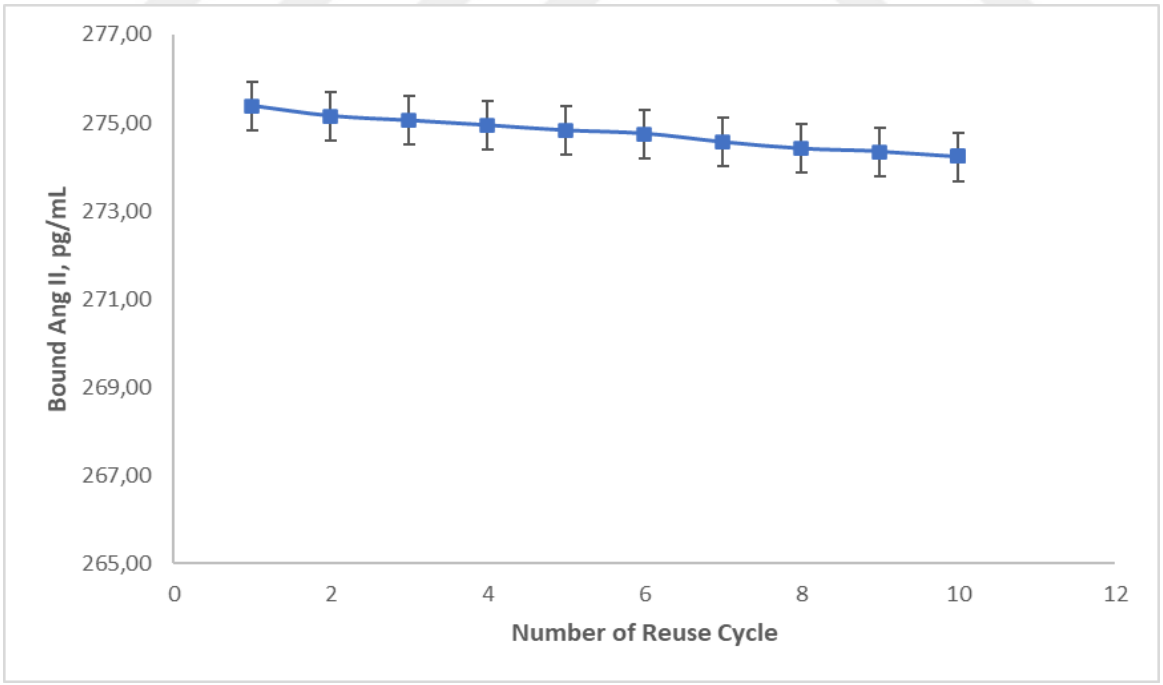

Figure 4.14. Reusability Studies. Equilibrium Ang II concentration: 50 pg/mL, mdry: 0.0754 g, V: 1,5 mL, pH 7.4, time: 120 min, rotating: 400 rpm, T: 25°C

4.7. Selective Ang II Rebinding From Human Serum Studies

Selective Ang II binding from human serum was performed in human serum testing by using 1:20-fold diluted serum. The diluted human serum sample was spiked with Ang II to 25 pg/mL and then the adsorption behavior was measured using ELISA. According to the obtained ELISA results the Ang II rebinding amount was found as 196 pg/g as 78.4% recovery. These resuts showed that the synthesized Ang II-MIPs$_{np}$ can recognize Ang II successfully even in complex media ie. human serum.

5. CONCLUSIONS

In this thesis, Ang II imprinted Hydroxyethyl methacrylate (HEMA) based nanoparticles were successfully synthesized by using miniemulsion polymerization reaction for sensitive and specific determination of Ang II from aqueous solutions. NPs were characterized after synthesis of Ang II-MIP_{np} and the control group NIP_{np}. Zeta Dimension Analysis, SEM, TEM and FTIR-ATR spectrophotometer analyzes were performed within the scope of characterization studies. As a result of the Zeta analysis, the particle sizes of Ang II-MIP_{np} and NIP_{np} were recorded as 50.25 and 51.97 nm, respectively. Specific surface areas were calculated as 26903.4 and 25868.9 m^2/g, respectively. SEM and TEM results also support a homogeneous polymerization and particle sizes obtained as a result of particle analysis. Adsorption of Ang II molecules was investigated in terms of their binding capacity to recognition sites, selectivity and reusability of nanoparticles were tested by kinetic studies. In adsorption studies, the effects of initial Ang II concentration, interaction time and temperature on Ang II adsorption were analyzed separately. As a result of the adsorption studies, it was observed that the Ang II adsorption of the synthesized NPs could drop down to 50 pg/mL sensitively. 0.5 M NaCl solution was used for desorption and 98% recovery was achieved. The adsorption-desorption cycle was repeated 10 times and no significant change was observed in the adsorption capacity. As a result of the selectivity studies, Ang I and Vsp molecules were used for Ang II-MIP_{np} and NIP_{np} and the dispersion and selectivity coefficients were calculated for Ang I and Vsp according to Ang II molecules. The selectivity coefficients for Ang II-MIP_{np} and NIP_{np}, respectively, were 2.75 and 0.54 for Ang I molecule; It was found to be 0.94 and 0.25 for Vsp. Relative selectivity coefficient showing the inhibition selectivity was calculated as 5.14 for Ang II/Ang I and 12.66 for Ang II/Vsp. Another definition; Ang II imprinted polymers had Ang II 5.14 times over Ang I; It recognizes with 12.66 fold selectivity compared to Vsp. Relative selectivity coefficients indicate the affinity of Ang II imprinted recognition sites.

As a result, within the scope of this thesis study, Ang II imprinted nanoparticles were developed, which has never been done before in the literature, in order to detect Ang II, which is a biomarker of many cardiovascular diseases, in a sensitive and selective way, and Ang II was successfully detected.

REFERENCES

Akhtar, K., Khan, S. A., Khan, S. B., & Asiri, A. M. (2018). Scanning electron microscopy: Principle and applications in nanomaterials characterization. In *Handbook of materials characterization* (pp. 113-145). Springer, Cham.

Albericio, F., & Tulla-Puche, J. (Eds.). (2008). *The power of functional resins in organic synthesis*. John Wiley & Sons.

Alexander, C., Andersson, H. S., Andersson, L. I., Ansell, R. J., Kirsch, N., Nicholls, I. A., ... & Whitcombe, M. J. (2006). Molecular imprinting science and technology: a survey of the literature for the years up to and including 2003. Journal of Molecular Recognition: An Interdisciplinary Journal, 19(2), 106-180.

Alvarez-Lorenzo, C., & Concheiro, A. (2004). Molecularly imprinted polymers for drug delivery. *Journal of Chromatography B*, *804*(1), 231-245.

Ames, M. K., Atkins, C. E., & Pitt, B. (2019). The renin-angiotensin-aldosterone system and its suppression. Journal of veterinary internal medicine, 33(2), 363-382.

Andaç, M., Baydemir, G., & Denizli, A. (2018). Molecularly imprinted polymers as a tool for biomolecule separation. *Nanoscale fabrication, optimization, scale-up and biological aspects of pharmaceutical nanotechnology*, 511-545.

Atlas, S. A. (2007). The renin-angiotensin-aldosterone system: pathophysiological role and pharmacologic inhibition. Journal of managed care pharmacy, 13(8 Supp B), 9-20.

Bader, M. (2010). Tissue renin-angiotensin-aldosterone systems: Targets for pharmacological therapy. Annual review of pharmacology and toxicology, 50, 439-465.

Bangs, L. B. (1987). Uniform Latex Particles Seradyn Inc. *Seragen Diagnostics Inc., Indianapolis, ABD*.

Battal, D., Akgönüllü, S., Yalçın, M. S., Yavuz, H., Denizli, A. 2018. "Molecularly imprinted polymer based quartz crystal microbalance sensor system for sensitive and label-free detection of synthetic cannabinoids in urine", Biosensors and Bioelectronics, 111, 10-17.

Bayda, S., Adeel, M., Tuccinardi, T., Cordani, M., & Rizzolio, F. (2019). The history of nanoscience and nanotechnology: from chemical–physical applications to nanomedicine. *Molecules*, *25*(1), 112.

Baydemir, G., Andaç, M., Derazshamshir, A., Uygun, D. A., Özçalışkan, E., Akgöl, S., & Denizli, A. (2013). Synthesis and characterization of amino acid containing Cu (II) chelated nanoparticles for lysozyme adsorption. *Materials Science and Engineering: C*, *33*(1), 532-536.

Behbahani, M., Taghizadeh, M., Bagheri, A., Hosseini, H., Salarian, M., & Tootoonchi, A. (2012). A nanostructured ion-imprinted polymer for the selective extraction and preconcentration of ultra-trace quantities of nickel ions. *Microchimica Acta*, *178*(3), 429-437.

Benigni, A., Cassis, P., & Remuzzi, G. (2010). Angiotensin II revisited: new roles in inflammation, immunology and aging. EMBO molecular medicine, 2(7), 247-257.

Bergmann, N. M., & Peppas, N. A. (2008). Molecularly imprinted polymers with specific recognition for macromolecules and proteins. Progress in Polymer Science, 33(3), 271-288.

Biçen, Ö. (2010). *Moleküler baskılanmış polimer tabanlı kriyojel ayırma sistemleri ve biyo-ayırma uygulamaları* (Doctoral dissertation, Anadolu University (Turkey)).

Bitas, D., & Samanidou, V. (2018). Molecularly imprinted polymers as extracting media for the chromatographic determination of antibiotics in milk. *Molecules*, *23*(2), 316.

Brewster, U. C., & Perazella, M. A. (2004). The renin-angiotensin-aldosterone system and the kidney: effects on kidney disease. The American journal of medicine, 116(4), 263-272.

Brewster, U. C., & Perazella, M. A. (2004). The renin-angiotensin-aldosterone system and the kidney: effects on kidney disease. *The American journal of medicine*, *116*(4), 263-272.

Brown, S. C., Palazuelos, M., Sharma, P., Powers, K. W., Roberts, S. M., Grobmyer, S. R., & Moudgil, B. M. (2010). Nanoparticle characterization for cancer nanotechnology and other biological applications. *Cancer Nanotechnology*, 39-65.

Catt, K. J., Cain, M. D., Zimmet, P. Z., & Cran, E. (1969). Blood angiotensin II levels of normal and hypertensive subjects. Br Med J, 1(5647), 819-821.

Chappell, M. C. (2016). Biochemical evaluation of the renin-angiotensin system: the good, bad, and absolute?. American Journal of Physiology-Heart and Circulatory Physiology, 310(2), H137-H152.

Chapuis, F., Pichon, V., & Hennion, M. C. (2004). Molecularly Imprinted Polymers: Developments and applications of new selective solid-phase extraction materials. *LC GC Europe*, 408-417.

Chen, L., Wang, X., Lu, W., Wu, X., & Li, J. (2016). Molecular imprinting: perspectives and applications. Chemical Society Reviews, 45(8), 2137-2211.

Ciraci, S., Ozbay, E., Gulseren, O., Demir, H. V., Bayindir, M., Oral, A., ... & Dana, A. (2005). TÜBITAK Science and Technology Booklet. *Nanotechnology in Turkey*.

Cocchi, M., Foca, G., Lucisano, M., Marchetti, A., Pagani, M. A., Tassi, L., & Ulrici, A. (2004). Classification of cereal flours by chemometric analysis of MIR spectra. *Journal of agricultural and food chemistry*, *52*(5), 1062-1067.

Colafella, K. M. M., Bovée, D. M., & Danser, A. J. (2019). The renin-angiotensin-aldosterone system and its therapeutic targets. Experimental eye research, 186, 107680.

Cormack, P. A., & Elorza, A. Z. (2004). Molecularly imprinted polymers: synthesis and characterisation. *Journal of chromatography B*, *804*(1), 173-182.

Cormack, P. A., & Mosbach, K. (1999). Molecular imprinting: recent developments and the road ahead. *Reactive and Functional Polymers*, *41*(1-3), 115-124.

Curcio, P., Zandanel, C., Wagner, A., Mioskowski, C., & Baati, R. (2009). Semi-Covalent Surface Molecular Imprinting of Polymers by One-Stage Mini-emulsion Polymerization: Glucopyranoside as a Model Analyte. Macromolecular bioscience, 9(6), 596-604.

ÇALIK, Ş., Ayşe, K. O. Ç., ŞENEL, T., Erhan, Z. O. R., & ASLAN, O. Nanobilim ve Nanoteknolojinin TÜBİTAK Popüler Bilim Dergilerine Yansımaları. *Uluslararası Türk Eğitim Bilimleri Dergisi*, *2021*(17), 90-113.

Çimen, D., & Denizli, A. (2020). Development of rapid, sensitive, and effective plasmonic nanosensor for the detection of vitamins in infact formula and milk samples. *Photonic Sensors*, *10*(4), 316-332.

Çorman, M. E. (2010). *Moleküler baskılanmış nanopartiküllerin hazırlanması, karakterizasyonu ve lizozim saflaştırılmasında kullanılması* (Master's thesis, Adnan Menderes Üniversitesi, Fen Bilimleri Enstitüsü).

Çorman, M. E., & Akgöl, S. (2012). Preparation of molecular imprinted hydrophobic polymeric nanoparticles having structural memories for lysozyme recognition. *Artificial Cells, Blood Substitutes, and Biotechnology*, *40*(4), 245-255.

Dai, J., Vu, D., Nagel, S., Lin, C. H., & Fidalgo de Cortalezzi, M. (2018). Colloidal crystal templated molecular imprinted polymer for the detection of 2-butoxyethanol in water contaminated by hydraulic fracturing. *Microchimica Acta*, *185*(1), 1-8.

Daniel, S., Rao, P. P., & Rao, T. P. (2005). Investigation of different polymerization methods on the analytical performance of palladium (II) ion imprinted polymer materials. *Analytica chimica acta*, *536*(1-2), 197-206.

Danser, A. J. (2003). Local renin–angiotensin systems: the unanswered questions. The international journal of biochemistry & cell biology, 35(6), 759-768.

Daoud-Attieh, M., Chaib, H., Armutcu, C., Uzun, L., Elkak, A., & Denizli, A. (2013). Immunoglobulin G purification from bovine serum with pseudo-specific supermacroporous cryogels. Separation and Purification Technology, 118, 816-822.

Demiralay, E. C., Andac, M., Say, R., Alsancak, G., & Denizli, A. (2010). Nickel (II)-imprinted monolithic columns for selective nickel recognition. *Journal of applied polymer science*, *117*(6), 3704-3714.

Dhand, C., Dwivedi, N., Loh, X. J., Ying, A. N. J., Verma, N. K., Beuerman, R. W., ... & Ramakrishna, S. (2015). Methods and strategies for the synthesis of diverse nanoparticles and their applications: a comprehensive overview. *Rsc Advances*, *5*(127), 105003-105037.

Doğan, M. (2005). Kimyada nanoteknoloji devri. *Kimya Teknolojileri Dergisi*, *57*, 20-24.

EREN, N. B. (2022). DÜNYADA VE TÜRKİYE'DE NANOTEKNOLOJİ. *SAĞLIK & BİLİM 2022: NANOTIP*, 7.

Ernst, A. U., Bowers, D. T., Wang, L. H., Shariati, K., Plesser, M. D., Brown, N. K., ... & Ma, M. (2019). Nanotechnology in cell replacement therapies for type 1 diabetes. *Advanced drug delivery reviews*, *139*, 116-138.

Ertürk, G., Özen, H., Tümer, M. A., Mattiasson, B., Denizli, A. 2016. "Microcontact imprinting based surface plasmon resonance (SPR) biosensor for real-time and ultrasensitive detection of prostate specific antigen (PSA) from clinical samples", Sensors and Actuators B: Chemical, 224, 823-832.

Fan, Y., Zeng, X., Yi, J., & Zhang, Y. (2020). Fabrication of pea protein nanoparticles with calcium-induced cross-linking for the stabilization and delivery of antioxidative resveratrol. *International journal of biological macromolecules*, *152*, 189-198.

Fasihi, J., Alahyari, S. A., Shamsipur, M., Sharghi, H., & Charkhi, A. (2011). Adsorption of uranyl ion onto an anthraquinone based ion-imprinted copolymer. *Reactive and Functional Polymers*, *71*(8), 803-808.

Fleming, I. (2006). Signaling by the angiotensin-converting enzyme. Circulation research, 98(7), 887-896.

Foo, K. Y., & Hameed, B. H. (2010). Insights into the modeling of adsorption isotherm systems. Chemical engineering journal, 156(1), 2-10.

Fu, Q., Sanbe, H., Kagawa, C., Kunimoto, K. K., & Haginaka, J. (2003). Uniformly sized molecularly imprinted polymer for (S)-nilvadipine. Comparison of chiral recognition ability with HPLC chiral stationary phases based on a protein. *Analytical chemistry*, *75*(2), 191-198.

Fyhrquist, F., & Saijonmaa, O. (2008). Renin-angiotensin system revisited. Journal of internal medicine, 264(3), 224-236.

Gao, M., Gao, Y., Chen, G., Huang, X., Xu, X., Lv, J., ... & Liu, G. (2020). Recent advances and future trends in the detection of contaminants by molecularly imprinted polymers in food samples. *Frontiers in Chemistry*, *8*, 616326.

Gheblawi, M., Wang, K., Viveiros, A., Nguyen, Q., Zhong, J. C., Turner, A. J., ... & Oudit, G. Y. (2020). Angiotensin-converting enzyme 2: SARS-CoV-2 receptor and regulator of the renin-angiotensin system: celebrating the 20th anniversary of the discovery of ACE2. Circulation research, 126(10), 1456-1474.

Goldberg, M. S. (2019). Improving cancer immunotherapy through nanotechnology. *Nature Reviews Cancer*, *19*(10), 587-602.

Goodsell, D. S. (2004). *Bionanotechnology: lessons from nature*. John Wiley & Sons.

Gosetti, F., Mazzucco, E., Zampieri, D., & Gennaro, M. C. (2010). Signal suppression/enhancement in high-performance liquid chromatography tandem mass spectrometry. Journal of Chromatography A, 1217(25), 3929-3937.

Gürmen, S., Ebin, B., & İtü, M. (2008). Nanopartiküller ve üretim yöntemleri-1. *Metalurji Dergisi*, *150*, 31-38.

Haupt, K., & Mosbach, K. (2000). Molecularly imprinted polymers and their use in biomimetic sensors. Chemical reviews, 100(7), 2495-2504.

He, S., Zhang, L., Bai, S., Yang, H., Cui, Z., Zhang, X., & Li, Y. (2021). Advances of molecularly imprinted polymers (MIP) and the application in drug delivery. *European Polymer Journal*, *143*, 110179.

He, X., Deng, H., & Hwang, H. M. (2019). The current application of nanotechnology in food and agriculture. *Journal of food and drug analysis*, *27*(1), 1-21.

Hu, Y., & Niemeyer, C. M. (2019). From DNA nanotechnology to material systems engineering. *Advanced Materials*, *31*(26), 1806294.

Idziak, I., Benrebouh, A., & Deschamps, F. (2001). Simple NMR experiments as a means to predict the performance of an anti-17α-ethynylestradiol molecularly imprinted polymer. *Analytica chimica acta*, *435*(1), 137-140.

Khan, I., Saeed, K., & Khan, I. (2019). Nanoparticles: Properties, applications and toxicities. *Arabian journal of chemistry*, *12*(7), 908-931.

Kobori, H., Katsurada, A., Miyata, K., Ohashi, N., Satou, R., Saito, T., ... & Navar, L. G. (2008). Determination of plasma and urinary angiotensinogen levels in rodents by newly developed ELISA. American Journal of Physiology-Renal Physiology, 294(5), F1257-F1263.

Li, L., Zhang, C., Chen, Y., & Liu, X. (2022). The use of nanoparticles for high-efficiency CO2 capture by methanol. *Journal of CO2 Utilization*, *66*, 102299.

Li, X., Husson, S.M., 2006. Adsorption of dansylated amino acids on molecularly imprinted surfaces: a surface plasmon resonance study. Biosensors and Bioelectronics, 22, 336-348.

Li, Y., Li, X., Li, Y., Dong, C., Jin, P., & Qi, J. (2009). Selective recognition of veterinary drugs residues by artificial antibodies designed using a computational approach. *Biomaterials*, *30*(18), 3205-3211.

Mahony, J. O., Nolan, K., Smyth, M. R., & Mizaikoff, B. (2005). Molecularly imprinted polymers—potential and challenges in analytical chemistry. Analytica chimica acta, 534(1), 31-39.

Miller, J. C., Serrato, R., Represas-Cardenas, J. M., & Kundahl, G. (2004). *The handbook of nanotechnology: Business, policy, and intellectual property law*. John Wiley & Sons.

Milunovich, S., John, M. A., & Fan, Z. (2004). Nanotech report. *Merrill Lynch Nanotech Index*.

Mitchell, M. J., Billingsley, M. M., Haley, R. M., Wechsler, M. E., Peppas, N. A., & Langer, R. (2021). Engineering precision nanoparticles for drug delivery. *Nature Reviews Drug Discovery*, *20*(2), 101-124.

Mohann, D., Pittman, C.U. Jr. and Steele, P.H. 2006. Single, binary and multicomponent adsorption of copper and cadmium from aqueous solutions on Kraft lignin-a biosorbent. Journal of Colloid and Interface Science, 297: 489-504.

Mondal, P., Anweshan, A., & Purkait, M. K. (2020). Green synthesis and environmental application of iron-based nanomaterials and nanocomposite: a review. *Chemosphere*, *259*, 127509.

Mondal, P., Anweshan, A., & Purkait, M. K. (2020). Green synthesis and environmental application of iron-based nanomaterials and nanocomposite: a review. *Chemosphere, 259,* 127509.

Montezano, A. C., Nguyen Dinh Cat, A., Rios, F. J., & Touyz, R. M. (2014). Angiotensin II and vascular injury. Current hypertension reports, 16, 1-11.

Morais, M. G. D., Martins, V. G., Steffens, D., Pranke, P., & da Costa, J. A. V. (2014). Biological applications of nanobiotechnology. *Journal of nanoscience and nanotechnology*, *14*(1), 1007-1017.

Mosbach, K., & Mosbach, R. O. L. F. (1966). Entrapment of enzymes and microorganisms in synthetic cross-linked polymers and their application in column techniques. Acta chem. scand, 20(10), 2807-2810.

Mosbach, K., & Ramström, O. (1996). The emerging technique of molecular imprinting and its future impact on biotechnology. Bio/technology, 14(2), 163-170.

Nadagouda, M. N., Speth, T. F., & Varma, R. S. (2011). Microwave-assisted green synthesis of silver nanostructures. *Accounts of Chemical Research*, *44*(7), 469-478.

Grubu, N. S. (2023). Nanobilim ve nanoteknoloji stratejileri.

Okay, O. (2000). Macroporous copolymer networks. *Progress in polymer science*, *25*(6), 711-779.

Otero-Romani, J., Moreda-Piñeiro, A., Bermejo-Barrera, P., & Martin-Esteban, A. (2008). Synthesis, characterization and evaluation of ionic-imprinted polymers for solid-phase extraction of nickel from seawater. *analytica chimica acta*, *630*(1), 1-9.

Özkara, S., Andaç, M., Karakoç, V., Say, R., & Denizli, A. (2011). Ion-imprinted PHEMA based monolith for the removal of Fe3+ ions from aqueous solutions. *Journal of applied polymer science*, *120*(3), 1829-1836.

Parisi, O. I., Francomano, F., Dattilo, M., Patitucci, F., Prete, S., Amone, F., & Puoci, F. (2022). The Evolution of Molecular Recognition: From Antibodies to Molecularly Imprinted Polymers (MIPs) as Artificial Counterpart. *Journal of Functional Biomaterials*, *13*(1), 12.

Parisi, O. I., Ruffo, M., Malivindi, R., Vattimo, A. F., Pezzi, V., & Puoci, F. (2020). Molecularly imprinted polymers (MIPs) as theranostic systems for sunitinib controlled release and self-monitoring in cancer therapy. *Pharmaceutics*, *12*(1), 41.

Pillai, G. (2019). Nanotechnology toward treating cancer: A comprehensive review. *Applications of targeted nano drugs and delivery systems*, 221-256.

Qi, P., Wang, J., Wang, L., Li, Y., Jin, J., Su, F., ... & Chen, J. (2010). Molecularly imprinted polymers synthesized via semi-covalent imprinting with sacrificial spacer for imprinting phenols. *Polymer*, *51*(23), 5417-5423.

Ramanathan, S., Gopinath, S. C., Arshad, M. M., Poopalan, P., & Perumal, V. (2021). Nanoparticle synthetic methods: strength and limitations. In *Nanoparticles in Analytical and Medical Devices* (pp. 31-43). Elsevier.

Rao, C. N. R., Müller, A., & Cheetham, A. K. (Eds.). (2006). *The chemistry of nanomaterials: synthesis, properties and applications*. John Wiley & Sons.

Rosenbaugh, E. G., Savalia, K. K., Manickam, D. S., & Zimmerman, M. C. (2013). Antioxidant-based therapies for angiotensin II-associated cardiovascular diseases. American Journal of Physiology-Regulatory, Integrative and Comparative Physiology, 304(11), R917-R928.

Sajid, M., & Płotka-Wasylka, J. (2020). Nanoparticles: Synthesis, characteristics, and applications in analytical and other sciences. *Microchemical Journal*, *154*, 104623.

Salata, O. V. (2004). Applications of nanoparticles in biology and medicine. *Journal of nanobiotechnology*, *2*(1), 1-6.

Scorrano, S., Mergola, L., Del Sole, R., & Vasapollo, G. (2011). Synthesis of molecularly imprinted polymers for amino acid derivates by using different functional monomers. *International journal of molecular sciences*, *12*(3), 1735-1743.

Sellergren, B., Lepistoe, M., & Mosbach, K. (1988). Highly enantioselective and substrate-selective polymers obtained by molecular imprinting utilizing noncovalent interactions. NMR

and chromatographic studies on the nature of recognition. *Journal of the American chemical society*, *110*(17), 5853-5860.

Sener, G., Ozgur, E., Yılmaz, E., Uzun, L., Say, R., & Denizli, A. (2010). Quartz crystal microbalance based nanosensor for lysozyme detection with lysozyme imprinted nanoparticles. *Biosensors and Bioelectronics*, *26*(2), 815-821.

Sircar, A., Rayavarapu, K., Bist, N., Yadav, K., & Singh, S. (2022). Applications of nanoparticles in enhanced oil recovery. *Petroleum Research*, *7*(1), 77-90.

Taguchi, H., Sunayama, H., Takano, E., Kitayama, Y., & Takeuchi, T. (2015). Preparation of molecularly imprinted polymers for the recognition of proteins via the generation of peptide-fragment binding sites by semi-covalent imprinting and enzymatic digestion. Analyst, 140(5), 1448-1452.

Tan, C. J., & Tong, Y. W. (2007). Molecularly imprinted beads by surface imprinting. *Analytical and bioanalytical chemistry*, *389*(2), 369-376.

Tekin, K., Uzun, L., Şahin, Ç. A., Bektaş, S., & Denizli, A. (2011). Preparation and characterization of composite cryogels containing imidazole group and use in heavy metal removal. Reactive and Functional Polymers, 71(10), 985-993.

Tikellis, C., & Thomas, M. C. (2012). Angiotensin-converting enzyme 2 (ACE2) is a key modulator of the renin angiotensin system in health and disease. International journal of peptides, 2012.

Turiel, E., Tadeo, J. L., Cormack, P. A. G., & Martin-Esteban, A. (2005). HPLC imprinted-stationary phase prepared by precipitation polymerisation for the determination of thiabendazole in fruit. *Analyst*, *130*(12), 1601-1607.

Unger, T. (2000). Neurohormonal modulation in cardiovascular disease. American Heart Journal, 139(1), s2-s8.

Voelker, J. R., Cobb, S. L., & Bowsher, R. R. (1994). Improved HPLC-radioimmunoassay for quantifying angiotensin II in plasma. Clinical chemistry, 40(8), 1537-1543.

Wang, N. X., & von Recum, H. A. (2011). Affinity-based drug delivery. *Macromolecular bioscience*, *11*(3), 321-332.

Weiss, C., Carriere, M., Fusco, L., Capua, I., Regla-Nava, J. A., Pasquali, M., ... & Delogu, L. G. (2020). Toward nanotechnology-enabled approaches against the COVID-19 pandemic. *ACS nano*, *14*(6), 6383-6406.

Whitcombe, M. J., Kirsch, N., & Nicholls, I. A. (2014). Molecular imprinting science and technology: a survey of the literature for the years 2004–2011. Journal of Molecular Recognition, 27(6), 297-401.

Wu, D., Zhou, J., Creyer, M. N., Yim, W., Chen, Z., Messersmith, P. B., & Jokerst, J. V. (2021). Phenolic-enabled nanotechnology: Versatile particle engineering for biomedicine. *Chemical Society Reviews*, *50*(7), 4432-4483.

Wulff, G. (1972). The use of polymers with enzyme-analogous structures for the resolution of racemates. Angrew. Chem. Internat. Edit., 11(4), 341.

Yaqoob, A. A., Ahmad, H., Parveen, T., Ahmad, A., Oves, M., Ismail, I. M., ... & Mohamad Ibrahim, M. N. (2020). Recent advances in metal decorated nanomaterials and their various biological applications: a review. *Frontiers in chemistry*, *8*, 341.

Yıldırım, M., & Baydemir Peşint, G. (2021). Molecularly imprinted spongy columns for Angiotensin (II) recognition from human serum. *Biotechnology Progress*, *37*(2), e3112.

Yılmaz, R., & Yunus, E. (2006). Anjiyotensin II reseptör blokerleri ve yeni bir ajan: olmesartan medoksomil. *Turk MedLine*, *13*, 176-82.

Yu, C., & Mosbach, K. (1997). Molecular imprinting utilizing an amide functional group for hydrogen bonding leading to highly efficient polymers. *The Journal of Organic Chemistry*, *62*(12), 4057-4064.

Zenger, O., & Peşint, G. B. (2022). Preparation of molecularly imprinted bilayer cryogel columns for selective protein depletion. *Process Biochemistry*, *117*, 90-100.

Zhang, L., Cheng, G., & Fu, C. (2002). Molecular selectivity of tyrosine-imprinted polymers prepared by seed swelling and suspension polymerization. *Polymer international, 51*(8), 687-692.

Melville, H. (1989). Hawthorne and his mosses. In N. Baym (Ed.), The Norton anthology of American literature (3rd ed., pp. 12-34). New York, NY: W.W. Norton & Company.